

1 We again thank the reviewer and editor for their constructive comments and we address their
2 various concerns below.

3

4 Response to Editor

5 The revised manuscript represents an improvement, but there are a few important points
6 raised by the Referee that are necessary before recommending that the present manuscript be
7 published in Biogeosciences. In addition to the comments by the Referee, Please consider
8 ways to make figures 3-7 more informative

9 In revision we did originally amend the figures, we removed the grey banding that
10 represented the drought period and instead added a second y-axis to show rainfall (or lack
11 thereof) during the summer of 2003. This should make it clearer to the reader when trying to
12 interpret the down-regulation of fluxes in responses to water stress. We have experimented
13 with many alternative ways to present the information in the figures, but ultimately it is
14 complicated as we are attempting to show six different lines. In revision we have now
15 changed the “no drought” line to a “dash-dot” black line. This removes the two shades of blue
16 in figures 3-7. We have also added information describing the different simulations to the
17 figure captions, e.g. “*Simulations show the control (CTRL) and the three parameterisations,*
18 *which represent a spectrum of behaviour ranging from high to low drought sensitivity (based*
19 *on Zhou et al. 2013; 2014), and the tested methods to obtain a weighted estimate of soil water*
20 *potential (Ψ_s) across CABLE's soil layers (M1-M3). M1 uses a root-biomass weighted soil*
21 *water content converted to Ψ_s , M2 calculates Ψ_s by integrated soil water content over the top*
22 *1.7m of the soil, and M3 is calculated using a dynamic weight across soil layers.”*

23

24 and please note carefully in the Discussion and Conclusions that the number of sites explored
25 somewhat limits the generality of the findings with an eye toward future research.

26 We have incorporated the Editor's suggestion about the limitations of our study into our
27 existing discussion text that broadly addressed this point:

28

29 “*Our work thus underlines a need to move beyond models that implement drought sensitivity*
30 *through a single PFT parameterisation. **Although we only compared vegetation at five sites,***

31 *it has been widely shown that species originating from different hydroclimates vary in their*
32 *drought sensitivities (Choat et al. 2012; Limousin et al. 2013; Zhou et al. 2014; Mitchell et*
33 *al., 2014; Mencuccini et al. 2015) and our results indicate that these differing sensitivities*
34 *at the plant level are also important at the ecosystem scale. It is, of course, challenging to*
35 *implement such a continuum of sensitivities in a global vegetation model. In this study, we*
36 *used a simple site-specific approach in which we selected three sets of model parameters from*
37 *a meta-analysis by Zhou et al. (2013; 2014), allowing us to characterise a range of plant*
38 *responses to drought. **The approach we tested in this paper could not be directly***
39 ***implemented in global vegetation models:** these models would require a more sophisticated*
40 *approach that relates drought sensitivity to the climate of each pixel. One potential solution*
41 *would be to develop an empirical correlation between drought sensitivity and a long-term*
42 *moisture index (e.g. the ratio of mean precipitation to the equilibrium evapotranspiration;*
43 *Cramer and Prentice, 1988; Gallego-Sala et al. 2010). Previous studies have demonstrated*
44 *the feasibility of linking model parameters that determine plant water use strategy to such a*
45 *moisture index in global simulations (Wang et al. 2014; De Kauwe et al. 2015). Such an*
46 *approach would requires a concerted effort to collate appropriate data, as there are few*
47 *compilations to date of traits related to drought sensitivity (but see Manzoni et al. 2011; Zhou*
48 *et al. 2013). Another, more challenging, alternative, would be to develop optimization*
49 *hypotheses that can predict vegetation drought sensitivity from climate (e.g. Manzoni et al.*
50 *2014).”*

51

52 **Please draft a short letter outlining any changes made, after which I will not hesitate to**
53 **recommend that the improved manuscript be published.**

54

55

56

57

58 Response to Reviewer

59

60 The paper is much improved and most of the criticisms in the reviews have been dealt with
61 effectively. I have one remaining issue with the results: Table 4 and 5 are crucial here. Results
62 are discussed on l. 1080 onwards, so there should be further references to these tables in this
63 paragraph.

64 All the numbers listed to support model improvement come directly from tables 4 and 5, we
65 now make this clearer by referring to both tables throughout the results.

66

67 The authors argue from their 5 site analysis that there is a trend towards better RMSE and
68 NSE from “high” to “low” parameters, matching the mesic to xeric shift. I can see this for LE
69 (table 4). However, this trend is not clear in GPP (table 5), where a ‘medium’ parameter set
70 works for 4 out of 5 sites. So the results are suggestive, but not as conclusive as the authors
71 argue. I think the discussion needs to address this issue directly.

72 We largely agree with the reviewer’s summary of the GPP result, which does not disagree
73 with the text we wrote. However, by summarising that the medium sensitivity worked best at
74 4/5 sites, it ignores the fact that at the most mesic end, the low sensitivity worked best
75 (Espirra) and the most mesic end (Tharandt), the high sensitivity ($\text{RMSE} = 2.23 \text{ g C m}^{-2} \text{ d}^{-1}$)
76 was very similar to the best performing medium sensitivity ($\text{RMSE} = 2.12 \text{ g C m}^{-2} \text{ d}^{-1}$).
77 Nevertheless, we now add the following text to the discussion: *“Whilst this characterisation
78 of the transition of drought sensitivities was largely consistent for both water and carbon
79 fluxes, it is notable for the two most mesic sites, a medium rather than a high drought
80 sensitivity performed best for carbon fluxes. There are a number of possible explanations;
81 however, as the relationships tested are not site-specific it is hard to be conclusive as to the
82 exact cause. Nevertheless, it does suggest that the parameterisation of the high drought
83 sensitivity may be too sensitive at mesic sites, which will need further investigation.”*

84

85 Table 4 and 5: currently their captions are too short; further details are required -explain all
86 the columns (e.g. high, medium, low); explain that sites are in order from mesic to xeric; three
87 significant figures would be sufficient for each data column. People rarely read an entire
88 paper, but will glance at figures and tables, so clear metadata are required.

89 We thank the reviewer for this suggestion and have improved table captions accordingly, for
90 example:

91
92
93
94
95
96
97
98
99
100
101
102
103
104
105
106
107
108
109
110
111
112
113
114
115
116

“Table 4: Summary statistics of modelled and observed latent heat (LE) at the five FLUXNET sites during the main drought period (1st of June – 31st August, 2003). The results of the three parameterisations, which represent a spectrum of behaviour, ranging from high to low drought sensitivity, are shown for the three tested approaches (M1-M3) to obtain a weighted estimate of soil water potential (Ψ_s) across CABLE's soil layers. M1 uses a root-biomass weighted soil water content converted to Ψ_s , M2 calculates Ψ_s by integrated soil water content over the top 1.7m of the soil, and M3 is calculated using a dynamic weighting across soil layers. Sites have been ordered to show a mesic-xeric transition between sites (Tharandt to Espirra). For each site the best performing model simulation has been highlighted in bold.”

I cannot find Table 2 referenced in the text.

Table 2 is referred to in the methods: “To assess the performance of the CABLE model both with and without the new drought scheme, we selected a gradient of five forested Fluxnet (<http://www.fluxdata.org/>) sites across Europe (Table 2) from those available through the Protocol for the Analysis of Land Surface models (PALS; pals.unsw.edu.au; Abramowitz, 2012).”

117 **Do land surface models need to include differential plant**
118 **species responses to drought? Examining model**
119 **predictions across a mesic-xeric gradient in Europe.**

120

121 **M. G. De Kauwe¹, S.-X. Zhou^{1,2}, B. E. Medlyn^{1,3}, A. J. Pitman⁴, Y.-P. Wang⁵, R. A.**
122 **Duursma³ and I. C. Prentice^{1,6}**

123

124 [1]{Macquarie University, Department of Biological Sciences, New South Wales 2109,
125 Australia.}

126 [2] {CSIRO Agriculture Flagship, Waite Campus, PMB 2, Glen Osmond, SA 5064,
127 Australia.}

128 [3]{Hawkesbury Institute for the Environment, Western Sydney University, Locked Bag
129 1797, Penrith, NSW, Australia}

130 [4]{Australian Research Council Centre of Excellence for Climate Systems Science and
131 Climate Change Research Centre, UNSW, Sydney, Australia}

132 [5]{CSIRO Ocean and Atmosphere Flagship, Private Bag #1, Aspendale, Victoria 3195,
133 Australia}

134 [6]{AXA Chair of Biosphere and Climate Impacts, Grand Challenges in Ecosystems and
135 the Environment and Grantham Institute – Climate Change and the Environment,
136 Department of Life Sciences, Imperial College London, Silwood Park Campus, Buckhurst
137 Road, Ascot SL5 7PY, UK}

138

139

140 Correspondence to: M. G. De Kauwe (mdekauwe@gmail.com)

141

142

143 **Abstract**

144 Future climate change has the potential to increase drought in many regions of the globe,
145 making it essential that land surface models (LSMs) used in coupled climate models,
146 realistically capture the drought responses of vegetation. Recent data syntheses show that
147 drought sensitivity varies considerably among plants from different climate zones, but state-
148 of-the-art LSMs currently assume the same drought sensitivity for all vegetation. We tested
149 whether variable drought sensitivities are needed to explain the observed large-scale patterns
150 of drought impact on the carbon, water and energy fluxes. We implemented data-driven
151 drought sensitivities in the Community Atmosphere Biosphere Land Exchange (CABLE)
152 LSM and evaluated alternative sensitivities across a latitudinal gradient in Europe during the
153 2003 heatwave. The model predicted an overly abrupt onset of drought unless average soil
154 water potential was calculated with dynamic weighting across soil layers. We found that high
155 drought sensitivity at the most mesic sites, and low drought sensitivity at the most xeric sites,
156 was necessary to accurately model responses during drought. Our results indicate that LSMs
157 will over-estimate drought impacts in drier climates unless different sensitivity of vegetation
158 to drought is taken into account.

159

160

161

162

163

164

165

166

167

168

169

170

171 **1 Introduction**

172 Changes in regional precipitation patterns with climate change are highly uncertain (Sillmann
173 et al. 2014), but are widely expected to result in a change in the frequency, duration and
174 severity of drought events (Allen et al. 2010). Drought is broadly defined, but for plants is a
175 marked deficit of moisture in the root zone which results from a period of low rainfall and/or
176 increased atmospheric demand for evapotranspiration. Recently, a series of high-profile
177 drought events (Ciais et al. 2005; Fensham et al. 2009; Phillips et al. 2009; Lewis et al. 2011)
178 and associated tree mortality (Breshears et al. 2005; van Mantgem et al. 2009; Peng et al.
179 2011; Anderegg et al. 2013), have occurred across the globe and these events have led to
180 debate as to whether incidence of drought are increasing (Allen et al. 2010; Dai et al. 2013,
181 but see Sheffield et al. 2012). Drought and any ensuing vegetation mortality events have the
182 potential to change land ecosystems from a sink to source (Lewis et al. 2011), and the
183 dominant mechanisms governing the ecosystem responses to drought can vary from reducing
184 stomatal conductance (Xu and Baldocchi, 2003) to increasing tree mortality (Lewis et al.
185 2011) and changing community species composition (Nepstad et al. 2007).

186
187 Our ability to model drought effect on vegetation function (carbon and water fluxes) is
188 currently limited (Galbraith et al. 2010; Egea et al. 2011; Powell et al. 2013). Remarkably,
189 given the importance of correctly capturing drought impacts on carbon and water fluxes, land
190 surface models (LSMs) designed for use in climate models have rarely been benchmarked
191 against extreme drought events. Mahfouf et al. (1996) compared summertime crop
192 transpiration from 14 land surface schemes, finding that only half of the models fell within the
193 uncertainty range of the observations. They attributed differences among models to the
194 various schemes used by models to represent transpiration processes (e.g. soil water stress
195 function, different number of soil layers) and variability in the initial soil water content at the
196 start of the growing season which relates to variability in the way bare soil evaporation and
197 drainage are represented among different models. Galbraith et al. (2010) showed that a set of
198 dynamic global vegetation models (DGVMs) were unable to capture the 20–30% reduction in
199 biomass due to drought during a set of throughfall exclusion experiments in the Amazon.
200 Galbraith et al. (2010) attributed model variability during drought to: changes in autotrophic
201 respiration (which was not supported by the data), model insensitivity to observed leaf area
202 reductions, and the use of different empirical functions to down-regulate productivity during

203 water stress. The models differed both in terms of time-scale of the application of this
204 function (sub-diurnal vs. daily) and whether it was used to down-regulate net photosynthesis
205 or the maximum rate of Rubisco activity, V_{cmax} . Similarly, Powell et al. (2013) demonstrated
206 that a group of five models were unable to predict drought-induced reductions in aboveground
207 biomass (~20%) in two large-scale Amazon experiments. Gerten et al. (2008) compared the
208 effect of adjusting precipitation regimes on simulated net primary productivity (NPP) by four
209 ecosystem models across a range of hydroclimates. They found a consistent direction of
210 change (in terms of NPP) with different scenarios across models but found that the seasonal
211 evolution of soil moisture differed among the models.

212

213 In order for models to better capture realistic responses during drought, they need to draw
214 more closely on experimental data (see Chaves et al. 1993 for a review). One key observation
215 is that there is a continuum of species responses to soil moisture deficit, ranging from
216 isohydric (stomata close rapidly during drought, maintaining a minimum leaf water potential,
217 Ψ_l) to anisohydric (stomata remain open during drought, which allows Ψ_l to decrease)
218 hydraulic strategies (Tardieu and Simonneau, 1998; Klein, 2014). These differences are
219 widely observed and are thought to be important in determining resilience to drought
220 (McDowell et al. 2008; Mitchell et al. 2013; Garcia-Forner et al. 2015). Many traits, including
221 hydraulic conductivity, resistance to cavitation, turgor loss point, stomatal regulation and
222 rooting depth, contribute to these differences. Systematic differences in the response of leaf
223 gas exchange to soil moisture potential have been observed among species originating from
224 different hydroclimates (Zhou et al. 2013), with species from mesic environments showing
225 stronger stomatal sensitivity to drought than species from xeric environments. Currently,
226 these environmental gradients in species behaviour are not captured in LSMs, which typically
227 assume static plant functional type (PFT) parameterisations. This is in part because
228 historically the data required to describe these attributes have not been available at the global
229 scale, but also due to the necessity of simplification required to run global climate model
230 simulations. Species with a PFT are assumed to have similar or identical sensitivities to
231 drought. Such an approach ignores experimental evidence of the range of sensitivities to
232 drought among species (Choat et al. 2012; Limousin et al. 2013; Zhou et al. 2014; Mitchell et
233 al., 2014; Mencuccini et al. 2015). For example, Turner et al. (1984) found contrasting
234 responses in leaf water potential to increasing vapour pressure deficit, ranging from isohydric

235 to anisohydric, among a group of woody and herbaceous species. Similarly, Zhou et al. (2014)
236 found that in a dry-down experiment, European sapling species originating from more mesic
237 environments were more sensitive to water stress (more rapid reduction of photosynthesis and
238 stomatal conductance) than species from more xeric regions. However, it is not known
239 whether observed differences in the response to soil moisture deficit among species are
240 important in determining fluxes at large scales.

241

242 In this study we test whether differences in species' responses to drought are needed to
243 capture drought responses on a continental scale. We built on recent changes to the stomatal
244 conductance (g_s) scheme (De Kauwe et al. 2015) within the Community Atmosphere
245 Biosphere Land Exchange (CABLE) LSM (Wang et al. 2011), by implementing a new
246 formulation for drought impacts based on plant ecophysiological studies for 31 species (Zhou
247 et al. 2013; 2014). We obtained three parameterisations for drought response from these
248 studies, characterising low, medium and high sensitivities to drought. We then applied
249 CABLE to simulate responses to an extreme meteorological event, the European 2003
250 heatwave, at five eddy covariance sites covering a latitudinal gradient, transitioning from
251 mesic sites at the northern extreme to xeric at the southern sites. Observations show that there
252 was a significant impact of drought on ecosystem fluxes at these sites (Ciais et al. 2005; Schär
253 et al. 2005). We note that models have been applied to simulate drought effects on
254 productivity (net primary production) and leaf area at individual sites (Ciais et al. 2005;
255 Fischer et al. 2007; Granier et al. 2007; Reichstein et al. 2007) but have not been used to
256 examine whether alternative parameterisations are needed to capture drought responses across
257 sites. We therefore tested how well CABLE was able to simulate the impact of drought on
258 carbon and water fluxes at these sites using alternative parameterisations for drought
259 sensitivity. We hypothesised that drought sensitivity would increase as sites transitioned from
260 xeric to mesic. We hypothesised that trees at more mesic sites, with a greater abundance of
261 available water than at xeric sites, would be more vulnerable to shorter duration droughts, and
262 thus have higher drought sensitivity (or lower resistance to drought). Therefore, accounting
263 for this latitudinal gradient in drought sensitivity would improve the performance of CABLE.

264 2 Methods

265 2.1 Model description

266 CABLE represents the vegetation using a single layer, two-leaf canopy model separated into
267 sunlit and shaded leaves (Wang and Leuning, 1998), with a detailed treatment of within
268 canopy turbulence (Raupach 1994; Raupach et al. 1997). Soil water and heat conduction is
269 numerically integrated over six discrete soil layers following the Richards equation and up to
270 three layers of snow can accumulate on the soil surface. A complete description can be found
271 in Kowalczyk et al. (2006) and Wang et al. (2011). CABLE has been used extensively for
272 both offline (Abramowitz et al. 2008; Wang et al. 2011; De Kauwe et al. 2015) and coupled
273 simulations (Cruz et al. 2010; Pitman et al. 2011; Mao et al. 2011; Lorenz et al. 2014) within
274 the Australian Community Climate Earth System Simulator (ACCESS, see
275 <http://www.accessimulator.org.au>; Kowalczyk et al. 2013); a fully coupled earth system
276 model. The source code can be accessed after registration at <https://trac.nci.org.au/trac/cable>.

277

278 2.2 Representing drought stress within CABLE.

279 We build on the work by De Kauwe et al. (2015), who introduced a new g_s scheme into
280 CABLE. In this scheme, stomata are assumed to behave optimally; that is, stomata are
281 regulated to maximise carbon gain whilst simultaneously minimising water loss, over short
282 time periods (i.e. a day) (Cowan and Farquhar, 1977) leading to the following formulation of
283 g_s (Medlyn et al. 2011)

$$g_s = g_0 + 1.6 \left(1 + \frac{g_1}{\sqrt{D}} \right) \frac{A}{C_s} \quad (1)$$

284 where A is the net assimilation rate ($\mu\text{mol m}^{-2} \text{s}^{-1}$), C_s ($\mu\text{mol mol}^{-1}$) and D (kPa) are the CO_2
285 concentration and the vapour pressure deficit at the leaf surface, respectively, and g_0 (mol m^{-2}
286 s^{-1}), and g_1 are fitted constants representing the residual stomatal conductance when A reaches
287 zero, and the slope of the sensitivity of g_s to A , respectively. The model was parameterised for
288 different PFTs using data from Lin et al. (2015) (see De Kauwe et al. 2015).

289

290 In the standard version of CABLE, drought stress is implemented as an empirical scalar (β)
 291 that depends on soil moisture content, weighted by the fraction of roots in each of CABLE's
 292 six soil layers:

$$\beta = \sum_{i=1}^n f_{root,i} \frac{\theta_i - \theta_w}{\theta_{fc} - \theta_w}; \beta \in [0,1] \quad (2)$$

293 where θ_i is the volumetric soil moisture content ($\text{m}^3 \text{m}^{-3}$) in soil layer i , θ_w is the wilting point
 294 ($\text{m}^3 \text{m}^{-3}$), θ_{fc} is the field capacity ($\text{m}^3 \text{m}^{-3}$) and $f_{root,i}$ is the fraction of root mass in soil layer
 295 i . The six soil layers in CABLE have depths 0.022 m, 0.058 m, 0.154 m, 0.409 m, 1.085 m
 296 and 2.872 m. The factor β is assumed to limit the slope of the relationship between stomatal
 297 conductance (g_s , $\text{mol m}^{-2} \text{s}^{-1}$; Leuning 1995) by acting as a modifier on the parameter g_1 .

298 In this study, we introduced a new expression for drought sensitivity of gas exchange, based
 299 on the work of Zhou et al. (2013, 2014). In this model, both g_1 and the photosynthetic
 300 parameters V_{cmax} and J_{max} are assumed to be sensitive to pre-dawn leaf water potential, but
 301 this sensitivity varies across species. There is considerable evidence that both g_1 and V_{cmax} are
 302 sensitive to soil moisture (Keenan et al. 2009; Egea et al. 2011; Flexas et al. 2012; Zhou et al.
 303 2013). There is also widespread evidence that plants more directly respond to water
 304 potential rather than water content (Comstock and Mencuccini 1998; Verhoef and Egea,
 305 2014).

306

307 Zhou et al. (2013) extended the optimal stomatal model of Medlyn et al. (2011) by fitting an
 308 exponential function to relate g_1 to pre-dawn leaf water potential (Ψ_{pd}):

$$g_1 = g_{1wet} \times \exp(b\Psi_{pd}) \quad (3)$$

309 where g_{1wet} is fitted parameter representing plant water use under well watered conditions (i.e.
 310 when $\Psi_{pd} = 0$) and b is a fitted parameter representing the sensitivity of g_1 to Ψ_{pd} . Species
 311 with different water use strategies can be hypothesised to differ in not only their g_1 parameter
 312 under well-watered conditions, g_{1wet} (see Lin et al. 2015), but also with the sensitivity to Ψ_{pd} ,
 313 b . Zhou et al. (2013) also advanced a non-stomatal limitation to the photosynthetic
 314 biochemistry, which describes the apparent effect of water stress on V_{cmax} :

$$V_{cmax} = V_{cmax,wet} \frac{1 + \exp(S_f \Psi_f)}{1 + \exp(S_f (\Psi_f - \Psi_{pd}))} \quad (4)$$

315 where $V_{cmax,wet}$ is the V_{cmax} value in well watered conditions, S_f is a sensitivity parameter
 316 describing the steepness of the decline with water stress, Ψ_f is the water potential at which
 317 Ψ_{pd} decreases to half of its maximum value. As with g_1 , it is hypothesised that in the same
 318 way species vary in their V_{cmax} values in well-watered conditions ($V_{cmax,wet}$), they would also
 319 differ in their sensitivity of down-regulated V_{cmax} with water stress (Zhou et al. 2014). In
 320 CABLE, as there is a constant ratio between the parameters J_{max} and V_{cmax} , the parameter J_{max}
 321 is similarly reduced by drought.

322

323 To implement Eq. (6) in CABLE we first had to convert soil moisture content (θ) to pre-dawn
 324 leaf water potential (Ψ_{pd}). We did so by assuming that overnight Ψ_{pd} and Ψ_s equilibrate
 325 before sunrise, thus ignoring any night-time transpiration (Dawson et al. 2007). Following
 326 Campbell (1974), we related θ to Ψ_s in each soil layer by:

$$\Psi_{s,i} = \Psi_e \left(\frac{\theta_i}{\theta_{sat}} \right)^{-k} \quad (5)$$

327 where Ψ_e is the air entry water potential (MPa) and k (unitless) is an empirical coefficient
 328 which is related to the soil texture. Values for Ψ_e and b are taken from CABLE's standard
 329 lookup table following Clapp and Hornberger (1978). We then needed to obtain a
 330 representative weighted estimate of Ψ_s across CABLE's soil layers. We tested three potential
 331 approaches for weighting in this paper:

- 332 (i) Using the root-biomass weighted θ and converting this to Ψ_s using Eq. (8),
 333 hereafter denoted M1. Such an approach is often favoured by models, following
 334 experimental evidence that plants preferentially access regions in the root zone
 335 where water is most freely available (Green and Clothier 1995; Huang et al. 1997).
- 336 (ii) Taking the integrated θ over the top 5 soil layers (1.7 m depth) and converting this
 337 to Ψ_s using Eq. (8), hereafter denoted M2. This method assumes the plant
 338 effectively has access to an entire "bucket" of soil water. This approach is often
 339 favoured by "simpler" forest productivity models (e.g. Landsberg and Waring,
 340 1997).

341 (iii) Weighting the average Ψ_s for each of the six soil layers by the weighted soil-to-
342 root conductance to water uptake of each layer, following Williams et al. (1996;
343 2001), hereafter denoted M3. The total conductance term depends the combination
344 of a soil component (R_s) and a root component (R_r). R_s is defined as (Gardner,
345 1960):

$$R_s = \frac{\ln\left(\frac{r_s}{r_r}\right)}{2\pi l_r D G_{soil}} \quad (6)$$

346 where r_s is the mean distance between roots (m), r_r is the fine root radius (m), D
347 is the depth of the soil layer, G_{soil} is the soil conductivity ($\text{mmol m}^{-1} \text{s}^{-1} \text{MPa}^{-1}$)
348 which depends on soil texture and soil water content, l_r is the fine root density
349 (mm^{-3}). R_r is defined as:

$$R_r = \frac{R_r^*}{FD} \quad (7)$$

350 where R_r^* is the root resistivity (MPa s g mmol^{-1}), F is the root biomass per unit
351 volume (g m^{-3}). This method weights Ψ_s to the upper soil layers when the soil is
352 wet, but shifts towards layer lowers as the soil dries, due to the lower soil
353 hydraulic conductance (e.g. Duursma et al. 2011).

354

355 2.3 Model simulations

356 During 2003, Europe experienced an anomalously dry summer, amplified by a combination of
357 a preceding dry spring and high summer temperatures (Ciais et al. 2005; Schär et al. 2005).
358 Summer temperatures were recorded to have exceeded the 30-year June-July-August (JJA)
359 average by 3°C (Schär et al. 2005). Consequently we choose to focus our model comparisons
360 on this period, in particular the period between June and September 2003.

361

362 At each of the five Fluxnet sites we ran three sets of simulations:

- 363 - A control simulation (“CTRL”), representing CABLE version 2.0.1.
- 364 - Three simulations to explore the new drought model using a “high” (*Quercus robur*),
365 “medium” (*Quercus ilex*) and “low” (*Cedrus atlantica*) sensitivity to soil moisture.

366 Parameter values were obtained from the meta-analysis by Zhou et al. (2013; 2014)
367 and are given in Table 1. For each of these simulations we also tested the three
368 different methods of obtaining Ψ_5 as described above.

369 - A “no drought” simulation in which any transpired water was returned to the soil. By
370 comparing this simulation with either the control or any of the new drought model
371 simulations (high, medium, low), a guide to the magnitude of the drought should be
372 apparent.

373

374 Model parameters were not calibrated to match site characteristics; instead default PFT
375 parameters were used for each site. Although CABLE has the ability to simulate full carbon,
376 nitrogen and phosphorus biogeochemical cycling, this feature was not activated for this study,
377 instead only the carbon and water cycle were simulated. For all simulations, leaf area index
378 (LAI) was prescribed using CABLE’s gridded monthly LAI climatology derived from
379 Moderate-resolution Imaging Spectroradiometer (MODIS) LAI data (Knyazikhin et al. 1998;
380 1999) and the g_s scheme following Medlyn et al. (2011; see De Kauwe et al. 2015) was used
381 throughout. All model simulations were spun-up by repeating the meteorological forcing site
382 data until soil moisture and soil temperatures reached equilibrium (as we were ignoring the
383 full biogeochemical cycling in these simulations).

384

385 **2.4 Datasets used**

386 To assess the performance of the CABLE model both with and without the new drought
387 scheme, we selected a gradient of five forested Fluxnet (<http://www.fluxdata.org/>) sites across
388 Europe (Table 2) from those available through the Protocol for the Analysis of Land Surface
389 models (PALS; pals.unsw.edu.au; Abramowitz, 2012). These data have previously been pre-
390 processed and quality controlled for use within the LSM community. Consequently, all site-
391 years had near complete observations of key meteorological drivers (as opposed to significant
392 gap-filled periods).

393

394 Model simulations were compared to measured latent heat and flux-derived gross primary
395 productivity (GPP) at each of the FLUXNET sites. Flux-derived GPP estimates are calculated

396 from the measured net ecosystem exchange (NEE) of carbon between the atmosphere and the
397 vegetation/soil, and the modelled ecosystem respiration (R_{eco}), where GPP is calculated as
398 $\text{NEE} + R_{\text{eco}}$.

399

400

401

402

403

404

405

406

407

408

409

410 3 Results

411 *Severity of the 2003 drought*

412 Table 3 summarises summer differences in rainfall, air temperature, GPP and LE between
413 2002 and 2003 across the five sites covering the latitudinal gradient from mesic to xeric sites
414 across Europe. Whilst the impact of the 2003 heatwave varied between sites, every site was
415 warmer and drier in 2003. Similarly, GPP was lower at every site except Espirra, and LE was
416 lower at three of the sites (Hesse, Roccarespampani and Castelporziano) in 2003 than in 2002.

417

418 *Simulated fluxes during drought from the standard model*

419 Figure 1 shows a site-scale comparison between standard CABLE (CTRL) transpiration (E),
420 flux derived GPP, and the observed LE at the five sites. Table 4 and 5 shows a series of
421 summary statistics (Root Mean Squared Error (RMSE), Nash-Sutcliffe efficiency (NSE),
422 Pearson's correlation coefficient (r) between modelled and observed GPP and LE. An
423 indication of the severity of the drought can be obtained by comparing the difference between
424 the "No drought" and the CTRL simulation.

425

426 For the two more mesic sites (Tharandt and Hesse), the CTRL simulation generally matched
427 the trajectory of the observed LE, but displayed systematic periods of over-estimation (i.e.
428 under-estimated the drought effect). By contrast, in the three more xeric sites
429 (Roccarespampani, Castelporziano and Espirra), the reverse was true: the CTRL simulations
430 descended into drought stress much more quickly than the observed fluxes. This rapid drought
431 progression was particularly evident around day of year 155 at the Roccarespampani site.
432 Across all sites, agreement with observed LE fluxes was generally poor (RMSE = 21.25 W m⁻²
433 to 38 W m⁻²; NSE = -8.95 to 0.15). This outcome is partly a result of the high soil
434 evaporation around mid-spring, which results in CABLE simulating very large LE fluxes
435 during this period.

436

437 At Tharandt, Hesse and Roccarespampani, simulated GPP systematically underestimated the
438 flux-derived peak GPP, particularly evident before day of year 180. Transitioning to the more
439 xeric sites (Roccarespampani, Castelporziano and Espirra), simulated GPP was apparently too

440 sensitive to water stress, contributing to a poor agreement with flux-derived data (RMSE =
441 2.22 g C m⁻² to 3.03 g C m⁻²; NSE = -2.67 to 0.42).

442

443 *Theoretical behaviour of new drought scheme*

444 We now consider the implementation of the new drought model and the three sensitivity
445 parameterisations. Figure 2a shows how leaf-level photosynthesis is predicted to decline
446 (using Eqs. 3 and 4) in the new drought model with increasing water stress (more negative
447 Ψ_s). The different sensitivities to drought are clearly visible, with the three parameterisations
448 representing a spectrum of behaviour ranging from high to low drought sensitivity. Figures 2b
449 and c show how the new drought model compares to the standard CABLE (CTRL; using Eq.
450 2) model on a sandy and clay soil type. The CTRL model is seen to most closely match the
451 high sensitivity simulation on a sandy soil, but it predicts an earlier descent into drought
452 stress. By contrast on the clay soil, the new medium and high sensitivity simulations
453 encompass the predictions from the CTRL model. The new drought model and
454 parameterisations afford a more flexible sensitivity to the down-regulation of photosynthesis
455 with drought, which is particularly evident in the low sensitivity simulation.

456

457 *Impact of new drought scheme on modelled LE*

458 Figures 3–7 show the same site comparisons as Fig. 1, but with the addition of the new
459 drought model and the three different ways (M1-3) in which Ψ_s can be averaged over the soil
460 profile. Across all sites it is clear that using M1, the new drought model behaves in much the
461 same way as the CTRL simulation. The explanation is that weighting Ψ_s by the fraction of
462 roots in each layer, results in water being principally extracted from the top three shallow
463 layers (Supplementary figures S1–S5). Consequently, small changes in θ result in a rapid
464 decline in Ψ_s (owing to the non-linear relationship between θ and Ψ_s , Fig. 1), which causes
465 an unrealistically abrupt shutdown of transpiration. M2 showed a greater separation between
466 the three sensitivity parameterisations than method one. The greater separation is most
467 evident at the xeric sites; the model performs particularly well at Espirra (LE RMSE < 16 W
468 m⁻² vs. CTRL RMSE = 35.31 W m⁻²) and to a lesser extent at Castelporziano (LE low
469 sensitivity RMSE = 19.72 W m⁻² vs. CTRL RMSE = 31.76 W m⁻²) (Table 4). Nevertheless, at
470 the two mesic sites, the model completely underestimates the size of the drought, as a result of

471 using a large soil water bucket (1.7 m) to calculate Ψ_5 . M3 in combination with the new
472 drought model generally performed the best across all the sites, as it allows CABLE to
473 simulate a more gradual reduction of fluxes during drought. At Roccarespampani a medium
474 drought sensitivity performed best at reproducing the observed LE (CTRL RMSE = 38.0 W
475 m^{-2} vs. 18.27 W m^{-2}), whilst at Espirra (CTRL RMSE = 35.31 W m^{-2} vs. 15.40 W m^{-2}) the
476 low sensitivity performed best (Table 4). At Castelporziano, both low (CTRL RMSE = 31.76
477 W m^{-2} vs. 20.41 W m^{-2}) and medium sensitivity (LE RMSE = 20.47 W m^{-2}) performed well
478 (Table 4). In contrast, at the two mesic sites, a high drought sensitivity performed best,
479 although at both Hesse (LE CTRL RMSE = 21.25 W m^{-2} vs. 25.90 W m^{-2}) and Tharandt (LE
480 CTRL RMSE = 28.5 W m^{-2} vs. 28.82 W m^{-2}), the new drought model performed marginally
481 worse than the CTRL (Table 4).

482

483 *Impact of new drought scheme on modelled GPP*

484 At the more xeric sites, there were noticeable improvements in simulated GPP during the
485 drought period (Figures 3–7). Similar to the LE result, across all sites M3 worked best (Table
486 5): using a medium drought sensitivity at both Roccarespampani (CTRL RMSE = 2.49 g C m^{-2}
487 d^{-1} vs. 1.73 g C m^{-2} d^{-1}) and Castelporziano (CTRL RMSE = 2.22 g C m^{-2} d^{-1} vs. 0.95 g C m^{-2}
488 d^{-1}), and a low sensitivity at Espirra (CTRL RMSE = 3.03 g C m^{-2} d^{-1} vs. 1.43 g C m^{-2} d^{-1}).
489 At the mesic end of the gradient, a medium sensitivity at Hesse (CTRL RMSE = 2.85 g C m^{-2}
490 d^{-1} vs. 2.71 g C m^{-2} d^{-1}) and a medium or high sensitivity at Tharandt worked best; although
491 using either sensitivity performed slightly worse than the CTRL (CTRL RMSE = 2.06 g C m^{-2}
492 d^{-1} vs. ≥ 2.23 g C m^{-2} d^{-1}) (Table 5).

493

494

495

496

497

498

499

Martin De Kauwe 7/12/2015 10:22 PM

Deleted: .

501 4 Discussion

502 Experimental data suggest that plants exhibit a continuum of drought sensitivities, with
503 species originating in more mesic environments showing higher sensitivity than species from
504 more xeric environments (Bahari et al. 1985; Reich and Hinckley, 1989; Ni and Pallardy,
505 1991; Zhou et al. 2014). We investigated whether variable drought sensitivity improves the
506 ability of the CABLE LSM to reproduce observed drought impacts across a latitudinal
507 gradient. We found that, at the mesic sites, a high drought sensitivity was required; moving
508 southwards towards more xeric sites, the sensitivity parameterisation transitioned to a medium
509 and finally to a low drought sensitivity. Whilst this characterisation of the transition of
510 drought sensitivities was largely consistent for both water and carbon fluxes, it is notable for
511 the two most mesic sites, a medium rather than a high drought sensitivity performed best for
512 carbon fluxes. There are a number of possible explanations; however, as the relationships
513 tested are not site-specific it is hard to be conclusive as to the exact cause. Nevertheless, it
514 does suggest that the parameterisation of the high drought sensitivity may be too sensitive at
515 mesic sites, which will need further investigation. This work demonstrates the importance of
516 understanding how plant traits vary with climate across the landscape. However, our analysis
517 also highlighted the importance of identifying which soil layers matter most to the plant: our
518 results depended strongly on how we weighted soil moisture availability through the profile.

519

520 *Weighting soil moisture availability*

521 Commonly, empirical dependences of gas exchange on soil moisture content or potential
522 (Eqns 3, 4) are estimated from pot experiments (e.g. Zhou et al. 2013; 2014), in which it is
523 fair to assume that the soil moisture content is relatively uniform and fully explored by roots.
524 In contrast, soil moisture content and rooting depth in the field typically have strong vertical
525 profiles. Thus, to implement such equations in a land surface model requires that we specify
526 how to weight the soil layers to obtain a representative value of whole-profile θ or Ψ_s . In this
527 study we tested three potential implementations. Our first approach was to weight each layer
528 by root biomass. Evidence suggests that plants preferentially access regions in the root zone
529 where water is most freely available (Green and Clothier 1995; Huang et al. 1997). Hence,
530 many models follow this approach: for example, the original version of CABLE weighted soil
531 moisture content by root biomass (Eqn 2) while the Community Land Model (CLM)

532 estimates a water stress factor based on a root-weighted Ψ_s , using a PFT-defined minimum
533 and maximum water potential (Oleson et al. 2013). However, we found that this approach
534 performed poorly. We observed an ‘on-off’ behaviour in response to drought, which occurs
535 because the behaviour of the model is driven by the top soil layers, whose total soil moisture
536 content is relatively small and root biomass is relatively high, and can be depleted rapidly,
537 leading to a sudden onset of severe drought. Many other LSMs show this abrupt effect of
538 drought (Egea et al., 2011; Powell et al., 2013). Powell et al. (2013) found that four models
539 (CLM version 3.5, Integrated Biosphere Simulator version 2.6.4 (IBIS), Joint UK Land
540 Environment Simulator version 2.1 (JULES), and Simple Biosphere model version 3 (SiB3))
541 implement abrupt transitions of this kind. We also found that with this weighting of soil
542 layers, there was little effect of variable drought sensitivity: the depletion of soil moisture
543 content of the top layers is so rapid that there is little difference between low and high
544 sensitivities to drought. Such an outcome suggests that there is little adaptive significance of
545 drought sensitivity, which seems unlikely. A further implication of using a root-weighted
546 function to calculate Ψ_s is that two distinctly different scenarios, a soil that has been very wet
547 but experienced a short dry period, allowing the topsoil to dry, and a soil that has had a
548 prolonged period of drought but experienced a recent rainfall event, would have similar
549 impacts on gas exchange. Again, this outcome seems unlikely.

550

551 We tested a second implementation in which soil moisture potential was calculated from the
552 moisture content of the entire rooting zone (top five soil layers = 1.7 m). Such an approach is
553 commonly used in forest productivity models (e.g. Landsberg and Waring, 1997). However,
554 this approach severely underestimates drought impacts because the moisture content of the
555 total soil profile is so large, meaning that it is rarely depleted enough to impact on gas
556 exchange.

557

558 In reality, plant water uptake shifts lower in the profile as soil dries out (e.g. Duursma et al.
559 2011). Thus, in our third implementation, we tested an approach in which the weighting of
560 soil layers moves downwards as drought progresses. This approach is effectively similar to
561 that used by the soil–plant–atmosphere (SPA) model (Williams et al. 1996; 2001), in which
562 soil layers are weighted by their soil-to-root conductance, which declines as the moisture

563 content declines. Of the three approaches we tested, this method performed best, allowing
564 CABLE to replicate the observations across the latitudinal mesic to xeric gradient. This
565 dynamic weighting of Ψ_s may partially explain previous good performance by SPA in other
566 model inter-comparisons focussed on drought (e.g. Powell et al. 2013). Recently, Bonan et al.
567 (2014) tested the suitability of using a model that considers optimal stomatal behaviour and
568 plant hydraulics (SPA; Williams et al. 1996) for earth system modelling, and demonstrated
569 marked improvement over the standard model during periods of drought stress. We thus
570 suggest that models using a soil moisture stress function to simulate drought effects on gas
571 exchange should consider a dynamic approach to weighting the contribution of different soil
572 layers.

573

574 We note that this issue is related to another long-standing problem for LSMs: that of
575 determining the vertical distribution of root water uptake (e.g. Feddes et al., 2001; Federer et
576 al., 2003; Kleidon and Heimann, 1998, 2000). In the standard version of CABLE, water
577 uptake from each soil layer initially depends on the fraction of root biomass in each layer, but
578 moves downwards during drought as the upper layers are depleted. It is possible that changes
579 to the weighting of soil moisture in determining drought sensitivity should also be
580 accompanied by changes to the distribution of root water uptake, but we did not explore this
581 option here. Li et al. (2012) previously tested an alternative dynamic root water uptake
582 function (Lai and Katul, 2000) in CABLE, but found little improvement in predicted LE
583 during seasonal droughts without also considering a mechanism for hydraulic redistribution.
584 Further work should evaluate models not only against LE fluxes, but also against
585 measurements of soil moisture profiles. Many experimental sites now routinely install
586 multiple soil moisture sensors (e.g. direct gravimetric sampling, neutron probes, time domain
587 reflectometry), which provide accurate insight into root water extraction and hydraulic
588 redistribution, even down to considerable depths (>4 m). These data have thus far been
589 underutilised for model improvement, but should be a priority for reducing the uncertainty in
590 soil moisture dynamics.

591

592 *Incorporating different sensitivities to drought*

593 Using the third and best method to calculate overall Ψ_s , we found that varying drought
594 sensitivity across sites enabled the model to better capture drought effects across the
595 mesic/xeric gradient, with a high drought sensitivity implied in mesic sites and a low drought
596 sensitivity implied in xeric sites. These results should not be surprising, given the increasing
597 amount of experimental evidence suggesting that drought sensitivity varies among species
598 and across climates (e.g. Engelbrecht and Kursar, 2003; Engelbrecht et al. 2007; Skelton et al.
599 2015). In contrast to these data, most LSMs assume a single parameterisation for drought
600 sensitivity, which is typically based on mesic vegetation. Our results suggest that such a
601 parameterisation is very likely to overstate the impacts of drought on both carbon and water
602 fluxes in drier regions.

603

604 Our work thus underlines a need to move beyond models that implement drought sensitivity
605 through a single PFT parameterisation. Although we only compared vegetation at five sites, it
606 has been widely shown that species originating from different hydroclimates vary in their
607 drought sensitivities (Choat et al. 2012; Limousin et al. 2013; Zhou et al. 2014; Mitchell et al.,
608 2014; Mencuccini et al. 2015) and our results indicate that these differing sensitivities at the
609 plant level are also important at the ecosystem scale. It is, of course, challenging to implement
610 such a continuum of sensitivities in a global vegetation model. In this study, we used a simple
611 site-specific approach in which we selected three sets of model parameters from a meta-
612 analysis by Zhou et al. (2013; 2014), allowing us to characterise a range of plant responses to
613 drought. The approach we tested in this paper could not be directly implemented in global
614 vegetation models: these models would require a more sophisticated approach that relates
615 drought sensitivity to the climate of each pixel. One potential solution would be to develop an
616 empirical correlation between drought sensitivity and a long-term moisture index (e.g. the
617 ratio of mean precipitation to the equilibrium evapotranspiration; Cramer and Prentice, 1988;
618 Gallego-Sala et al. 2010). Previous studies have demonstrated the feasibility of linking model
619 parameters that determine plant water use strategy to such a moisture index in global
620 simulations (Wang et al. 2014; De Kauwe et al. 2015). Such an approach would require a
621 concerted effort to collate appropriate data, as there are few compilations to date of traits
622 related to drought sensitivity (but see Manzoni et al. 2011; Zhou et al. 2013). Another, more
623 challenging, alternative, would be to develop optimization hypotheses that can predict
624 vegetation drought sensitivity from climate (e.g. Manzoni et al. 2014).

Martin De Kauwe 7/12/2015 2:00 PM

Deleted: In order to capture the observed variability in plant responses to drought, models need to consider a continuum of sensitivities.

Martin De Kauwe 5/12/2015 10:15 AM

Deleted: G

630

631 *Further model uncertainties*

632 Whilst this work advances the ability of LSMs to simulate drought, it does not address all
633 processes needed to correctly capture drought impacts. Other issues to consider include: (i)
634 rooting depth; (ii) leaf shedding; (iii) soil evaporation; and (iv) soil heterogeneity, among
635 others.

636

637 Here we have assumed that all sites had the soil depth (4.6 m), with rooting depth distributed
638 exponential through the profile, as is commonly used in LSMs. However, this assumption
639 may be incorrect. Access to water by deep roots could be a potential alternative explanation
640 for the low drought sensitivity that we inferred at the southernmost (xeric) site, Espirra. Here
641 the dominant species is not native to the region, but rather a plantation of blue gum
642 (*Eucalyptus globulus*), a species that is generally found to have high, not low, drought
643 sensitivity (White 1996; Mitchell et al. 2014). Many eucalypts have a deep rooting strategy
644 (Fabiao et al. 1987), suggesting a possible alternative explanation for drought tolerance at this
645 site. More in-depth study of fluxes and soil moisture patterns at this site would be needed to
646 determine the role of rooting depth.

647

648 During droughts, plants are often observed to shed their leaves. This is a self-regulatory
649 mechanism to reduce water losses (Tyree et al. 1993; Jonasson et al. 1997; Bréda et al. 2006).
650 During the 2003 heatwave at Hesse, an early reduction of approximately $1.7 \text{ m}^2 \text{ m}^{-2}$ was
651 observed. Similarly, at Brasschaat there was a observed reduction of $0.8 \text{ m}^2 \text{ m}^{-2}$ and at
652 Tharandt needle-litter was increased during September until November, with LAI estimated to
653 be $0.9 \text{ m}^2 \text{ m}^{-2}$ lower (Bréda et al. 2006; Granier et al. 2007). In contrast, models typically fix
654 turnover rates for leaves and as such this feedback is largely absent from models. During
655 periods of water stress, models do simulate an indirect reduction in LAI via down-regulated
656 net primary productivity, but this feedback is much slower than is commonly observed. Not
657 accounting for this canopy-scale feedback will result in models over-estimating carbon and
658 water fluxes and thus losses in θ during drought.

659

660 Existing models also disagree as to the mechanism by which to down-regulate productivity
661 during periods of water stress (De Kauwe et al. 2013). In the standard version of CABLE,
662 only the slope of the relationship between g_s and A is reduced by water stress. The SPA model
663 behaves similarly. In contrast, JULES (Clark et al. 2011) and the Sheffield Dynamic Global
664 Vegetation Model (SDGVM; Woodward and Lomas, 2004), down-regulate the
665 photosynthetic capacity via the biochemical parameters V_{cmax} and J_{max} (maximum electron
666 transport rate). Here, we assumed that water stress affects both the slope of g_s - A and the
667 biochemical parameters V_{cmax} and J_{max} , supported by results from Zhou et al. (2013, 2014).
668 We did not evaluate this assumption against the eddy flux data. However, previous studies
669 have also suggested that both effects are needed to explain responses of fluxes during drought
670 (Keenan et al. 2010).

671

672 Finally, although models do have the capacity to simulate vertical variations in θ , they do not
673 always represent horizontal sub-grid scale variability. This assumption is likely to contribute
674 to the abruptness of modelled transitions from well-watered to completely down-regulated
675 carbon and water fluxes. Earlier work by Entekhabi and Eagleson (1989), and models such as
676 the variable infiltration capacity (VIC) model (Liang et al. 1994), and most recently Decker
677 2015 (submitted) have attempted to address this issue by employing statistical distributions to
678 approximate horizontal spatial heterogeneity in soil moisture (see also Crow and Wood,
679 2002). These parsimonious approaches typically require few parameters, making them
680 attractive in the LSM context and potentially suitable for modelling ecosystem and
681 hydrological responses to drought (Luo et al. 2013).

682

683 *Testing models against extreme events*

684 In conclusion, we have used a model evaluation against flux measurements during a large-
685 scale heatwave event to make significant progress in modelling of drought impacts. While
686 model evaluation against data is now commonplace (Prentice et al. 2015) and has recently
687 been extended to formal benchmarking, particularly in the land surface community
688 (Abramowitz, 2005; Best et al. 2015), many of these benchmarking indicators are based on
689 seasonal or annual outputs and thus miss the opportunity to examine model performance
690 during extreme events. Model projections under future climate change require good

691 mechanistic representations of the impacts of extreme events. However, responses to extreme
692 events are rarely evaluated and there is therefore an urgent need to orient model testing to
693 periods of extremes. To that end, precipitation manipulation experiments (e.g. Nepstad et al.
694 2002; Hanson et al. 2003; Pangle et al. 2012) represent a good example of a currently under-
695 exploited avenue (but see Fisher et al. 2007; Powell et al. 2013) that could be used for model
696 evaluation and/or benchmarking (Smith et al. 2014). However, we urge that these exercises do
697 not focus solely on overall model performance, but also test the realism of individual model
698 assumptions (Medlyn et al. 2015).

699

700

701

702

703

704

705

706

707

708

709

710

711

712

713

714

715

716

717

718 **Acknowledgements**

719 This work was supported by the Australian Research Council (ARC) Linkage grant
720 LP140100232 and the ARC Centre of Excellence for Climate System Science
721 (CE110001028). SZ was supported by an international Macquarie University Research
722 Excellence Scholarship. This work is also a contribution to the AXA Chair Programme in
723 Biosphere and Climate Impacts and the Imperial College initiative on Grand Challenges in
724 Ecosystems and the Environment. We thank CSIRO and the Bureau of Meteorology through
725 the Centre for Australian Weather and Climate Research for their support in the use of the
726 CABLE model. This work used eddy covariance data acquired by the FLUXNET community
727 for the La Thuile FLUXNET release, supported by the following networks: AmeriFlux (U.S.
728 Department of Energy, Biological and Environmental Research, Terrestrial Carbon Program
729 (DE-FG02-04ER63917 and DE-FG02-04ER63911)), AfriFlux, AsiaFlux, CarboAfrica,
730 CarboEuropeIP, CarboItaly, CarboMont, ChinaFlux, Fluxnet-Canada (supported by CFCAS,
731 NSERC, BIOCAP, Environment Canada, and NRCan), GreenGrass, KoFlux, LBA, NECC,
732 OzFlux, TCOS-Siberia, USCCC. We acknowledge the financial support to the eddy
733 covariance data harmonization provided by CarboEuropeIP, FAO-GTOS-TCO, iLEAPS, Max
734 Planck Institute for Biogeochemistry, National Science Foundation, University of Tuscia,
735 Université Laval and Environment Canada and US Department of Energy and the database
736 development and technical support from Berkeley Water Center, Lawrence Berkeley National
737 Laboratory, Microsoft Research eScience, Oak Ridge National Laboratory, University of
738 California - Berkeley, University of Virginia. All data analysis and plots were generated using
739 the Python language and the Matplotlib plotting library (Hunter, 2007).

740

741

742

743

744

745

746

747

748 **References**

749 Abramowitz, G.: Towards a benchmark for land surface models, *Geophys. Res. Lett.*, 32,
750 L22702, 2005.

751

752 Abramowitz, G.: Towards a public, standardized, diagnostic benchmarking system for land
753 surface models, *Geosci. Model Dev.*, 5, 819–827, 2012.

754

755 Abramowitz, G., Leuning, R., Clark, M. and Pitman, A.: Evaluating the Performance of Land
756 Surface Models, *J. Clim.*, 21, 5468–5481, 2008.

757

758 Allen, C. D., Macalady, A. K., Chenchouni, H., Bachelet, D., McDowell, N., Vennetier, M.,
759 Kitzberger, T., Rigling, A., Breshears, D. D., Hogg, E. H. (Ted), Gonzalez, P., Fensham, R.,
760 Zhang, Z., Castro, J., Demidova, N., Lim, J.-H., Allard, G., Running, S. W., Semerci, A. and
761 Cobb, N.: A global overview of drought and heat-induced tree mortality reveals emerging
762 climate change risks for forests, *For. Ecol. Manag.*, 259, 660–684, 2010.

763

764 Anderegg, W. R., Kane, J. M. and Anderegg, L. D.: Consequences of widespread tree
765 mortality triggered by drought and temperature stress, *Nat. Clim. Change*, 3, 30–36, 2013.

766

767 Bahari, Z. A., Pallardy, S. G. and Parker, W.C. Photosynthesis, water relations, and drought
768 adaptation in six woody species of oak-hickory forests in central Missouri. *For. Sci.* 31:557-
769 569, 1985.

770

771 Best, M. J., Abramowitz, G., Johnson, H. R., Pitman, A. J., Balsamo, G. and Boone, A.,
772 Cuntz, M., Decharme, B., Dirmeyer, P. A., Dong, J., Ek, M., Guo, Z., Haverd, V., van den
773 Hurk, B. J. J., Nearing, G. S., Pak, B., Peters-Lidard, C., Santanello Jr., J. A., Stevens, L. and
774 Vuichard, N.: The Plumbing of Land Surface Models: Benchmarking Model Performance. *J.*
775 *Hydrometeor.* 16, 1425–1442, 2015.

776

777 Bonan, G., Williams, M., Fisher, R. and Oleson, K.: Modeling stomatal conductance in the
778 Earth system: linking leaf water-use efficiency and water transport along the soil-plant-
779 atmosphere continuum, *Geosci. Model Dev.*, 7, 2193–2222, 2014.

780

781 Bréda, N., Huc, R., Granier, A. and Dreyer, E.: Temperate forest trees and stands under severe
782 drought: a review of ecophysiological responses, adaptation processes and long-term
783 consequences, *Ann. For. Sci.*, 63, 625–644, 2006.

784

785 Breshears, D. D., Cobb, N. S., Rich, P. M., Price, K. P., Allen, C. D., Balice, R. G., Romme,
786 W. H., Kastens, J. H., Floyd, M. L., Belnap, J., Anderson, J. J., Myers, O. B. and Meyer, C.
787 W.: Regional vegetation die-off in response to global-change-type drought, *Proc. Natl. Acad.*
788 *Sci. U. S. A.*, 102, 15144–15148, 2005.

789

790 Campbell, G. S.: A simple method for determining unsaturated conductivity from moisture
791 retention data., *Soil Sci.*, 117, 311–314, 1974.

792

793 Canadell, J., Jackson, R., Ehleringer, J., Mooney, H., Sala, O. and Schulze, E.-D.: Maximum
794 rooting depth of vegetation types at the global scale, *Oecologia*, 108, 583–595, 1996.

795

796 Chaves, M. M., Maroco, J. P. and Pereira, J. S.: Understanding plant responses to drought—
797 from genes to the whole plant, *Funct. Plant Biol.*, 30, 239–264, 2003.

798

799 Choat, B., Jansen, S., Brodribb, T. J., Cochard, H., Delzon, S., Bhaskar, R., Bucci, S. J., Feild,
800 T. S., Gleason, S. M., Hacke, U. G., Jacobsen, A. L., Lens, F., Maherali, H., Martinez-Vilalta,
801 J., Mayr, S., Mencuccini, M., Mitchell, P. J., Nardini, A., Pittermann, J., Pratt, R. B., Sperry,
802 J. S., Westoby, M., Wright, I. J. and Zanne, A. E.: Global convergence in the vulnerability of
803 forests to drought, *Nature*, 491, 752–755, 2012.

804

805 Ciais, P., Reichstein, M., Viovy, N., Granier, A., Ogee, J., Allard, V., Aubinet, M.,
806 Buchmann, N., Bernhofer, C., Carrara, A., Chevallier, F., De Noblet, N., Friend, A. D.,
807 Friedlingstein, P., Grunwald, T., Heinesch, B., Keronen, P., Knohl, A., Krinner, G., Loustau,

808 D., Manca, G., Matteucci, G., Miglietta, F., Ourcival, J. M., Papale, D., Pilegaard, K.,
809 Rambal, S., Seufert, G., Soussana, J. F., Sanz, M. J., Schulze, E. D., Vesala, T. and Valentini,
810 R.: Europe-wide reduction in primary productivity caused by the heat and drought in 2003,
811 Nature, 437, 529–533, 2005.

812

813 Clapp, R. B. and Hornberger, G. M.: Empirical equations for some soil hydraulic properties,
814 Water Resour. Res., 14, 601–604, 1978.

815

816 Clark, D. B., Mercado, L. M., Sitch, S., Jones, C. D., Gedney, N., Best, M. J., Pryor, M.,
817 Rooney, G. G., Essery, R. L. H., Blyth, E., Boucher, O., Harding, R. J., Huntingford, C. and
818 Cox, P. M.: The Joint UK Land Environment Simulator (JULES), model description - Part 2:
819 Carbon fluxes and vegetation dynamics, Geosci. Model Dev., 4, 701–722, 2011.

820

821 Comstock, J. and Mencuccini, M.: Control of stomatal conductance by leaf water potential in
822 *Hymenoclea salsola* (T. & G.), a desert subshrub, Plant Cell Environ., 21, 1029–1038, 1998.

823

824 Cowan, I. and Farquhar, G.: Stomatal function in relation to leaf metabolism and
825 environment., in Society for Experimental Biology Symposium, Integration of Activity in the
826 Higher Plant, vol. 31, edited by D. H. Jennings, pp. 471–505, Cambridge University Press.,
827 1977.

828

829 Cramer, W. and Prentice, I.: Simulation of regional soil moisture deficits on a European scale,
830 Nor. Geogr. Tidsskr. - Nor. J. Geogr., 42, 149–151, 1988.

831

832 Crow, W. T and Wood, E. F.: Impact of soil moisture aggregation on surface energy flux
833 prediction during SGP'97. Geophys. Res. Lett., 29, 8-1, 2002.

834

835 Cruz, F. T., Pitman, A. J. and Wang, Y.-P.: Can the stomatal response to higher atmospheric
836 carbon dioxide explain the unusual temperatures during the 2002 Murray-Darling Basin
837 drought?, J. Geophys. Res. Atmospheres, 115(D2), 2010.

838
839 Dai, A.: Increasing drought under global warming in observations and models, *Nat. Clim.*
840 *Change*, 3, 52–58, 2013.

841
842 Dawson, T. E., Burgess, S. S., Tu, K. P., Oliveira, R. S., Santiago, L. S., Fisher, J. B.,
843 Simonin, K. A. and Ambrose, A. R.: Nighttime transpiration in woody plants from contrasting
844 ecosystems, *Tree Physiol.*, 27, 561–575, 2007.

845
846 Decker, M., A new Soil Moisture and Runoff Parameterization for the CABLE LSM
847 including subgrid scale processes, *J. Adv. Model Earth Sy.*, submitted, 2015.

848
849 De Kauwe, M. G., Medlyn, B. E., Zaehle, S., Walker, A. P., Dietze, M. C., Hickler, T., Jain,
850 A. K., Luo, Y., Parton, W. J., Prentice, I. C., Smith, B., Thornton, P. E., Wang, S., Wang, Y.-
851 P., Waarind, D., Weng, E., Crous, K. Y., Ellsworth, D. S., Hanson, P. J., Seok Kim, H.,
852 Warren, J. M., Oren, R. and Norby, R. J.: Forest water use and water use efficiency at
853 elevated CO₂: a model-data intercomparison at two contrasting temperate forest FACE sites,
854 *Glob. Change Biol.*, 19, 1759–1779, 2013.

855
856 De Kauwe, M. G., Kala, J., Lin, Y.-S., Pitman, A. J., Medlyn, B. E., Duursma, R. A.,
857 Abramowitz, G., Wang, Y.-P. and Miralles, D. G.: A test of an optimal stomatal conductance
858 scheme within the CABLE land surface model, *Geosci. Model Dev.*, 8, 431–452, 2015.

859
860 Duursma, R., Kolari, P., Perämäki, M., Nikinmaa, E., Hari, P., Delzon, S., Loustau, D.,
861 Ilvesniemi, H., Pumpanen, J. and Mäkelä, A.: Predicting the decline in daily maximum
862 transpiration rate of two pine stands during drought based on constant minimum leaf water
863 potential and plant hydraulic conductance, *Tree Physiol.*, 28, 265–276, 2008.

864
865 Duursma, R. A., Barton, C. V. M., Eamus, D., Medlyn, B. E., Ellsworth, D. S., Forster, M. A.,
866 Tissue, D. T., Linder S., McMurtrie, R. E. Rooting depth explains [CO₂] × drought interaction
867 in *Eucalyptus saligna*. *Tree Physiol.*, 31, 922–931, 2011.

868

869 Egea, G., Verhoef, A. and Vidale, P. L.: Towards an improved and more flexible
870 representation of water stress in coupled photosynthesis–stomatal conductance models, *Agric.*
871 *For. Meteorol.*, 151, 1370–1384, 2011.

872

873 Engelbrecht, B. M. J., Comita, L. S., Condit, R., Kursar, T. A., Tyree, M. T., Turner, B. L.,
874 Hubbell, S. P.: Drought sensitivity shapes species distribution patterns in tropical forests.
875 *Nature*, 447, 80-82.

876 Engelbrecht, B. M. J. and Kursar, T. A. Comparative drought-resistance of seedlings of 28
877 species of co-occurring tropical woody plants. *Oecologia*, 136, 383–393, 2003.

878

879 Entekhabi, D. and Eagleson, P. S.: Land surface hydrology parameterization for atmospheric
880 general circulation models including subgrid scale spatial variability, *J. Clim.*, 2, 816–831,
881 1989.

882

883 Fabião A., Madeira M., Steen E.: Root mass in plantations of *Eucalyptus globulus* in Portugal
884 in relation to soil characteristics. *Arid Soil Res. Rehabil* 1, 185-194, 1987.

885

886 Feddes, R. A., Hoff, H., Bruen, M., Dawson, T., de Rosnay, P., Dirmeyer, P., Jackson, R. B.,
887 Kabat, P., Kleidon, A., Lilly, A. and Pitman, A. J.: Modeling root water uptake in
888 hydrological and climate models, *Bull. Am. Meteorol. Soc.*, 82, 2797–2809, 2001.

889

890 Federer, C., Vörösmarty, C. and Fekete, B.: Sensitivity of annual evaporation to soil and root
891 properties in two models of contrasting complexity, *J. Hydrometeorol.*, 4, 1276–1290, 2003.

892

893 Fensham, R., Fairfax, R. and Ward, D.: Drought-induced tree death in savanna, *Glob. Change*
894 *Biol.*, 15, 380–387, 2009.

895

896 Fischer, E., Seneviratne, S., Lüthi, D. and Schär, C.: Contribution of land-atmosphere
897 coupling to recent European summer heat waves, *Geophys. Res. Lett.*, 34, 2007.

898

899 Flexas, J., Barbour, M. M., Brendel, O., Cabrera, H. M., Carriquí, M., Díaz-Espejo, A.,
900 Douthe, C., Dreyer, E., Ferrio, J. P., Gago, J., Gallé, A., Galmés, J., Kodama, N., Medrano,
901 H., Niinemets, Ü., Peguero-Pina, J. J., Pou, A., Ribas-Carbó, M., Tomás, M., Tosens, T. and
902 Warren, C. R.: Mesophyll diffusion conductance to CO₂: an unappreciated central player in
903 photosynthesis, *Plant Sci.*, 193, 70–84, 2012.

904

905 Galbraith, D., Levy, P. E., Sitch, S., Huntingford, C., Cox, P., Williams, M. and Meir, P.:
906 Multiple mechanisms of Amazonian forest biomass losses in three dynamic global vegetation
907 models under climate change, *New Phytol.*, 187, 647–665, 2010.

908

909 Gallego-Sala, A., Clark, J., House, J., Orr, H., Prentice, I. C., Smith, P., Farewell, T. and
910 Chapman, S.: Bioclimatic envelope model of climate change impacts on blanket peatland
911 distribution in Great Britain, *Clim. Res.*, 45, 151–162, 2010.

912

913 Garcia-Forner, N., Adams, H. D., Sevanto, S., Collins, A. D., Dickman, L. T., Hudson, P. J.,
914 Zeppel, M., Martínez-Vilalta, J. and McDowell, N. G.: Responses of two semiarid conifer tree
915 species to reduced precipitation and warming reveal new perspectives for stomatal regulation,
916 *Plant Cell Amp Environ.*, in press, 2015.

917

918 Gerten, D., Luo, Y., Le Maire, G., Parton, W. J., Keough, C., Weng, E., Beier, C., Ciais, P.,
919 Cramer, W., Dukes, J. S., Hanson, P. J., Knapp, A. A. K., Linder, S., Nepstad, D., Rustad, L.
920 and Sowerby, A.: Modelled effects of precipitation on ecosystem carbon and water dynamics
921 in different climatic zones, *Glob. Change Biol.*, 14, 2365–2379, 2008.

922

923 Green, S. R. and Clothier, B. E.: Root water uptake by kiwifruit vines following partial
924 wetting of the root zone. *Plant Soil*, 173, 317-328, 1995.

925

926 Hanson, P. J., M. A. Huston, and D. E. Todd: Walker branch throughfall displacement
927 experiment, in *North American Temperate Deciduous Forest Responses to Changing*

928 Precipitation Regimes, edited by P. J. Hanson and S. D. Wullschleger, pp. 8–31, Springer,
929 New York, 2003.

930

931 Huang, B., R. R. Duncan, and R. N. Carrow (1997), Drought-resistance mechanisms of seven
932 warm-season turfgrasses under surface soil drying: II. Root aspects, *Crop Sci.*, 37, 1863–
933 1869.

934

935 Hunter, J. D.: Matplotlib: A 2D graphics environment, *Comput. Sci. Amp Eng.*, 9, 90–95,
936 2007.

937

938 Keenan, T., García, R., Friend, A., Zaehle, S., Gracia, C. and Sabate, S.: Improved
939 understanding of drought controls on seasonal variation in Mediterranean forest canopy CO₂
940 and water fluxes through combined in situ measurements and ecosystem modelling,
941 *Biogeosciences*, 6, 1423–1444, 2009.

942

943 Keenan, T., Sabate, S. and Gracia, C.: The importance of mesophyll conductance in
944 regulating forest ecosystem productivity during drought periods, *Glob. Change Biol.*, 16,
945 1019–1034, 2010.

946

947 Kleidon, A. and Heimann, M.: A method of determining rooting depth from a terrestrial
948 biosphere model and its impacts on the global water and carbon cycle, *Glob. Change Biol.*, 4,
949 275–286, 1998.

950

951 Klein, T.: The variability of stomatal sensitivity to leaf water potential across tree species
952 indicates a continuum between isohydric and anisohydric behaviours, *Funct. Ecol.*, 28, 1313–
953 1320, 2014.

954

955 Knyazikhin, Y., Marshak, J. V., Diner, D. J., B, M. R., Verstraete, M., B, P. and Gobron, N.:
956 Estimation of vegetation canopy leaf area index and fraction of absorbed photosynthetically

957 active radiation from atmosphere-corrected MISR data, *J. Geophys. Res.*, 103, 32239–32257,
958 1998.

959

960 Knyazikhin, Y., Glassy, J., Privette, J. L., Tian, Y., Lotsch, A., Zhang, Y., Wang, Y.,
961 Morisette, J. T., P.Votava, Myneni, R. B., Neman, R. R. and Running, S. W.: MODIS Leaf
962 Area Index (LAI) and Fraction of Photosynthetically Active Radiation Absorbed by
963 Vegetation (FPAR) Product (MOD15) Algorithm Theoretical Basis Document. [online]
964 Available from: <http://eosps0.gsfc.nasa.gov/atbd/modistables.html>, 1999.

965

966 Kowalczyk, E., Stevens, L., Law, R., Dix, M., Wang, Y., Harman, I., Haynes, K., Srbinovsky,
967 J., Pak, B. and Ziehn, T.: The land surface model component of ACCESS: description and
968 impact on the simulated surface climatology, *Aust Meteorol Ocean. J.*, 63, 65–82, 2013.

969

970 Kowalczyk, E. A., Wang, Y. P., Wang, P., Law, R. H. and Davies, H. L.: The CSIRO
971 Atmosphere Biosphere Land Exchange (CABLE) model for use in climate models and as an
972 offline model, CSIRO, 2006.

973

974 Lai, C. T. and Katul, G.: The dynamic role of root-water uptake in coupling potential to actual
975 transpiration, *Adv. Water Resour.*, 23, 427–439, 2000.

976

977 Landsberg, J. and Waring, R.: A generalised model of forest productivity using simplified
978 concepts of radiation-use efficiency, carbon balance and partitioning, *For. Ecol. Manag.*, 95,
979 209–228, 1997.

980

981 Leuning, R.: A critical appraisal of a combined stomatal-photosynthesis model for C₃ plants.,
982 *Plant Cell Environ.*, 18, 339–355, 1995.

983

984 Lewis, S. L., Brando, P. M., Phillips, O. L., van der Heijden, G. M. and Nepstad, D.: The
985 2010 amazon drought, *Science*, 331, 554–554, 2011.

986

987 Li, L., Wang, Y.-P., Yu, Q, Pak, B., Eamus, D., Yan, J., van Gorsel, E. and Baker, I. T.:
988 Improving the responses of the Australian community land surface model (CABLE) to
989 seasonal drought. *J. Geophys. Res-Bioge.*, 117, G4, 2012.

990

991 Liang, X., Lettenmaier, D. P., Wood, E. F. and Burges, S. J.: A simple hydrologically based
992 model of land surface water and energy fluxes for general circulation models, *J. Geophys.*
993 *Res.- Ser.-*, 99, 14–415, 1994.

994

995 Limousin, J.-M., Bickford, C. P., Dickman, L. T., Pangle, R. E., Hudson, P. J., Boutz, A. L.,
996 Gehres, N., Osuna, J. L., Pockman, W. T. and McDowell, N. G.: Regulation and acclimation
997 of leaf gas exchange in a piñon-juniper woodland exposed to three different precipitation
998 regimes, *Plant Cell Environ.*, 36, 1812–1825, 2013.

999

1000 Lin, Y.-S., Medlyn, B. E., Duursma, R. A., Prentice, I. C., Wang, H., Baig, S., Eamus, D., de
1001 Dios, V. R., Mitchell, P., Ellsworth, D. S., de Beeck, M. O., Wallin, G., Uddling, J.,
1002 Tarvainen, L., Linderson, M.-L., Cernusak, L. A., Nippert, J. B., Ocheltree, T. W., Tissue, D.
1003 T., Martin-StPaul, N. K., Rogers, A., Warren, J. M., De Angelis, P., Hikosaka, K., Han, Q.,
1004 Onoda, Y., Gimeno, T. E., Barton, C. V. M., Bennie, J., Bonal, D., Bosc, A., Low, M.,
1005 Macinins-Ng, C., Rey, A., Rowland, L., Setterfield, S. A., Tausz-Posch, S., Zaragoza-
1006 Castells, J., Broadmeadow, M. S. J., Drake, J. E., Freeman, M., Ghannoum, O., Hutley, L. B.,
1007 Kelly, J. W., Kikuzawa, K., Kolari, P., Koyama, K., Limousin, J.-M., Meir, P., Lola da Costa,
1008 A. C., Mikkelsen, T. N., Salinas, N., Sun, W. and Wingate, L.: Optimal stomatal behaviour
1009 around the world, *Nat. Clim. Change*, 5, 459–464, 2015.

1010

1011 Lorenz, R., Pitman, A., Donat, M., Hirsch, A., Kala, J., Kowalczyk, E., Law, R. and
1012 Srbinovsky, J.: Representation of climate extreme indices in the ACCESS1. 3b coupled
1013 atmosphere-land surface model, *Geosci. Model Dev.*, 7, 545–567, 2014.

1014

1015 Luo, X., Liang, X., and McCarthy, H. R.: VIC+ for water-limited conditions: a study of
1016 biological and hydrological processes and their interactions in the soil-plant-atmosphere
1017 continuum, *Water Resour. Res.*, 49, 7711-7732, 2013.

1018
1019 Mahfouf, J.-F., Ciret, C., Ducharne, A., Irannejad, P., Noilhan, J., Shao, Y., Thornton, P.,
1020 Xue, Y. and Yang, Z.-L.: Analysis of transpiration results from the RICE and PILPS
1021 workshop, *Glob. Planet. Change*, 13, 73–88, 1996.

1022
1023 Manzoni, S.: Integrating plant hydraulics and gas exchange along the drought-response trait
1024 spectrum. *Tree Physiol*, 34, 1031-1034, 2014.

1025
1026 Manzoni, S., Vico, G., Katul, G., Fay, P. A., Polley, W., Palmroth, S. and Porporato, A.
1027 Optimizing stomatal conductance for maximum carbon gain under water stress: a meta-
1028 analysis across plant functional types and climates. *Funct. Ecol.*, 25, 456-467, 2011.

1029
1030 Mao, J., Pitman, A. J., Phipps, S. J., Abramowitz, G. and Wang, Y.: Global and regional
1031 coupled climate sensitivity to the parameterization of rainfall interception, *Clim. Dyn.*, 37,
1032 171–186, 2011.

1033
1034 McDowell, N., Pockman, W. T., Allen, C. D., Breshears, D. D., Cobb, N., Kolb, T., Plaut, J.,
1035 Sperry, J., West, A., Williams, D. G. and others: Mechanisms of plant survival and mortality
1036 during drought: why do some plants survive while others succumb to drought?, *New Phytol.*,
1037 178, 719–739, 2008.

1038
1039 McDowell, N. G. and Allen, C. D.: Darcy’s law predicts widespread forest mortality under
1040 climate warming, *Nat. Clim. Change*, 5, 669–672, 2015.

1041
1042 Medlyn, B. E. and Zaehle, S. and De Kauwe, M. G. and Walker, A. P. and Dietze, M. C. and
1043 Hanson, P. J. and Hickler, T. and Jain, A. K. and Luo, Y. and Parton, W. and Prentice, I. C.
1044 and Thornton, P. E. and Wang, S. and Wang, Y.-P. and Weng, E. and Iversen, C. M. and
1045 McCarthy, H. R. and Warren, J. M. and Oren, R. and Norby, R. J.: Using ecosystem
1046 experiments to improve vegetation models. *Nature Clim. Change*, 5, 528-534, 2015.

1047

1048 Medlyn, B. E., Duursma, R. A., Eamus, D., Ellsworth, D. S., Prentice, I. C., Barton, C. V. M.,
1049 Crous, K. Y., De Angelis, P., Freeman, M. and Wingate, L.: Reconciling the optimal and
1050 empirical approaches to modelling stomatal conductance, *Glob. Change Biol.*, 17, 2134–2144,
1051 2011.

1052

1053 Mencuccini, M., Minunno, F., Salmon, Y., Martínez-Vilalta, J. and Hölttä, T.: Coordination
1054 of physiological traits involved in drought-induced mortality of woody plants, *New Phytol.*, in
1055 press, 2015.

1056

1057 Milly, P.: Sensitivity of greenhouse summer dryness to changes in plant rooting
1058 characteristics, *Geophys. Res. Lett.*, 24, 269–271, 1997.

1059

1060 Mitchell, P., O’Grady, A., Tissue, D., Worledge, D. and Pinkard, E.: Co-ordination of growth,
1061 gas exchange and hydraulics define the carbon safety margin in tree species with contrasting
1062 drought strategies, *Tree Physiol.*, 34, 443–458, 2014.

1063

1064 Mitchell, P. J., O’Grady, A. P., Tissue, D. T., White, D. A., Ottenschlaeger, M. L. and
1065 Pinkard, E. A.: Drought response strategies define the relative contributions of hydraulic
1066 dysfunction and carbohydrate depletion during tree mortality, *New Phytol.*, 197, 862–872,
1067 2013.

1068

1069 Nepstad, D. C., Tohver, I. M., Ray, D., Moutinho, P. and Cardinot, G.: Mortality of large
1070 trees and lianas following experimental drought in an Amazon forest, *Ecology*, 88, 2259–
1071 2269, 2007.

1072

1073 Nepstad, D. C. and Moutinho, P. and Dias-Filho, M. B. and Davidson, E. and Cardinot, G.
1074 and Markewitz, D. and Figueiredo, R. and Vianna, N. and Chambers, J. and Ray, D. and
1075 Guerreiros, J. B. and Lefebvre, P. and Sternberg, L. and Moreira, M. and Barros, L. and
1076 Ishida, F. Y. and Tohver, I. and Belk, E. and Kalif, K. and Schwalbe, K.: The effects of
1077 partial throughfall exclusion on canopy processes, aboveground production, and
1078 biogeochemistry of an Amazon forest, *J. Geophys. Res.*, 107(D20), 8085, 2156-2202, 2002.

1079

1080 Ni, B.-R., and S. G. Pallardy. Response of gas exchange to water stress in seedlings of
1081 woody angiosperms. *Tree Physiol.*, 8, 1–9, 1991.

1082

1083 Oleson, K. W., Lawrence, D. M., Bonan, G. B., Drewniak, B., Huang, M., Koven, C. D.,
1084 Levis, S., Li, F., Riley, W. J., Subin, Z. M., Swenson, S. C., Thornton, P. E., Bozbiyik, A.,
1085 Fisher, R., Heald, C. L., Kluzek, E., Lamarque, J.-F., Lawrence, P. J., Leung, L. R.,
1086 Lipscomb, W., Muszala, S., Ricciuto, D. M., Sacks, W., Sun, Y., Tang, J. and Yang, Z.-L.:
1087 Technical Description of version 4.5 of the Community Land Model (CLM), NCAR
1088 Technical Note, Citeseer, National Center for Atmospheric Research, P.O. Box 3000,
1089 Boulder, Colorado., 2013.

1090

1091 Pangle, R. E., J. P. Hill, J. A. Plaut, E. A. Yopez, J. R. Elliot, N. Gehres, N. G. McDowell,
1092 and W. T. Pockman: Methodology and performance of a rainfall manipulation experiment in
1093 a piñon–juniper woodland, *Ecosphere*, 3, art28, 2012.

1094

1095 Peng, C., Ma, Z., Lei, X., Zhu, Q., Chen, H., Wang, W., Liu, S., Li, W., Fang, X. and Zhou,
1096 X.: A drought-induced pervasive increase in tree mortality across Canada's boreal forests,
1097 *Nat. Clim. Change*, 1, 467–471, 2011.

1098

1099 Phillips, O. L., Aragão, L. E. O. C., Lewis, S. L., Fisher, J. B., Lloyd, J., López-González, G.,
1100 Malhi, Y., Monteagudo, A., Peacock, J., Quesada, C. A., van der Heijden, G., Almeida, S.,
1101 Amaral, I., Arroyo, L., Aymard, G., Baker, T. R., Bánki, O., Blanc, L., Bonal, D., Brando, P.,
1102 Chave, J., de Oliveira, Á. C. A., Cardozo, N. D., Czimczik, C. I., Feldpausch, T. R., Freitas,
1103 M. A., Gloor, E., Higuchi, N., Jiménez, E., Lloyd, G., Meir, P., Mendoza, C., Morel, A.,
1104 Neill, D. A., Nepstad, D., Patiño, S., Peñuela, M. C., Prieto, A., Ramírez, F., Schwarz, M.,
1105 Silva, J., Silveira, M., Thomas, A. S., Steege, H. ter, Stropp, J., Vásquez, R., Zelazowski, P.,
1106 Dávila, E. A., Andelman, S., Andrade, A., Chao, K.-J., Erwin, T., Di Fiore, A., C., E. H.,
1107 Keeling, H., Killeen, T. J., Laurance, W. F., Cruz, A. P., Pitman, N. C. A., Vargas, P. N.,
1108 Ramírez-Angulo, H., Rudas, A., Salamão, R., Silva, N., Terborgh, J. and Torres-Lezama, A.:
1109 Drought sensitivity of the Amazon rainforest, *Science*, 323, 1344–1347, 2009.

1110
1111 Pitman, A., Avila, F., Abramowitz, G., Wang, Y., Phipps, S. and de Noblet-Ducoudré, N.:
1112 Importance of background climate in determining impact of land-cover change on regional
1113 climate, *Nat. Clim. Change*, 1, 472–475, 2011.

1114
1115 Powell, T. L., Galbraith, D. R., Christoffersen, B. O., Harper, A., Imbuzeiro, H. M. A.,
1116 Rowland, L., Almeida, S., Brando, P. M., da Costa, A. C. L., Costa, M. H., Levine, N. M.,
1117 Malhi, Y., Saleska, S. R., Sotta, E., Williams, M., Meir, P. and Moorcroft, P. R.: Confronting
1118 model predictions of carbon fluxes with measurements of Amazon forests subjected to
1119 experimental drought, *New Phytol.*, 200, 350–365, 2013.

1120
1121 Raupach, M.: Simplified expressions for vegetation roughness length and zero-plane
1122 displacement as functions of canopy height and area index, *Bound.-Layer Meteorol.*, 71, 211–
1123 216, 1994.

1124
1125 Raupach, M., Finkelde, K. and Zhang, L.: SCAM (Soil-Canopy-Atmosphere Model):
1126 Description and comparison with field data, *Aspendale Aust. CSIRO CEM Tech. Rep.*, (132),
1127 81, 1997.

1128 Reich, P. B. and T. M. Hinckley. Influence of pre-dawn water potential and soil-to-leaf
1129 hydraulic conductance on maximum daily leaf diffusive conductance in two oak species.
1130 *Funct. Ecol.* 3:719-126, 1989.

1131
1132 Reichstein, M., Ciais, P., Papale, D., Valentini, R., Running, S., Viovy, N., Cramer, W.,
1133 Granier, A., Ogée, J., Allard, V., Aubinet, M., Bernhofer, C., Buchmann, N., Carrara, A.,
1134 Grünwald, T., Heimann, M., Heinesch, B., Knohl, A., Kutsch, W., Loustau, D., Manca, G.,
1135 Matteucci, G., Miglietta, F., Ourcival, J. M., Pilegaard, K., Pumpanen, J., Rambal, S.,
1136 Schaphoff, S., Seufert, G., Soussana, J.-F., Sanz, M.-J., Vesala, T. and Zhao, M.: Reduction of
1137 ecosystem productivity and respiration during the European summer 2003 climate anomaly: a
1138 joint flux tower, remote sensing and modelling analysis, *Glob. Change Biol.*, 13, 634–651,
1139 2007.

1140

1141 Schär, C., Vidale, P. L., Lüthi, D., Frei, C., Häberli, C., Liniger, M. A. and Appenzeller, C.:
1142 The role of increasing temperature variability in European summer heatwaves, *Nature*, 427,
1143 332–336, 2004.

1144

1145 Sheffield, J., Wood, E. F. and Roderick, M. L.: Little change in global drought over the past
1146 60 years, *Nature*, 491, 435–438, 2012.

1147

1148 Skelton, R. P., West, A. G. and Dawson, T. E.: Predicting plant vulnerability to drought in
1149 biodiverse regions using functional traits, 112, 5744-5749, 2015.

1150

1151 Smith, N. G., Rodgers, V. L., Brzostek, E. R., Kulmatiski, A., Avolio, M. L., Hoover, D. L.,
1152 Koerner, S. E., Grant, K., Jentsch, A. and Fatichi, S., Niyogi, D.: Toward a better integration
1153 of biological data from precipitation manipulation experiments into Earth system models,
1154 *Rev. of Geophys.*, 52, 1944-9208, 2014.

1155

1156 Tardieu, F. and Simonneau, T.: Variability among species of stomatal control under
1157 fluctuating soil water status and evaporative demand: modelling isohydric and anisohydric
1158 behaviours, *J. Exp. Bot.*, 49, 419–432, 1998.

1159

1160 Tyree, M., Cochard, H., Cruiziat, P., Sinclair, B. and Ameglio, T.: Drought-induced leaf
1161 shedding in walnut: evidence for vulnerability segmentation, *Plant Cell Environ.*, 16, 879–
1162 882, 1993.

1163

1164 van Mantgem, P. J., Stephenson, N. L., Byrne, J. C., Daniels, L. D., Franklin, J. F., Fulé, P.
1165 Z., Harmon, M. E., Larson, A. J., Smith, J. M., Taylor, A. H. and others: Widespread increase
1166 of tree mortality rates in the western United States, *Science*, 323, 521–524, 2009.

1167

1168 Verhoef, A. and Egea, G.: Modeling plant transpiration under limited soil water: Comparison
1169 of different plant and soil hydraulic parameterizations and preliminary implications for their
1170 use in land surface models, *Agric. For. Meteorol.*, 191, 22–32, 2014.

1171

1172 Wang, H., Prentice, I. and Davis, T.: Biophysical constraints on gross primary production by
1173 the terrestrial biosphere, *Biogeosciences*, 11, 5987–6001, 2014.

1174

1175 Wang, Y. P. and Leuning, R.: A two-leaf model for canopy conductance, photosynthesis and
1176 partitioning of available energy I::: Model description and comparison with a multi-layered
1177 model, *Agric. For. Meteorol.*, 91, 89–111, 1998.

1178

1179 Wang, Y. P., Kowalczyk, E., Leuning, R., Abramowitz, G., Raupach, M. R., Pak, B., van
1180 Gorsel, E. and Luhar, A.: Diagnosing errors in a land surface model (CABLE) in the time and
1181 frequency domains, *J. Geophys. Res. Biogeosciences* 2005–2012, 116, 2011.

1182

1183 White, D.: Physiological responses to drought of *Eucalyptus globulus* and *Eucalyptus nitens*
1184 in plantations. PhD diss., University of Tasmania, 1996.

1185

1186 Williams, M., Rastetter, E. B., Fernandes, D. N., Goulden, M. L., Wofsy, S. C. and Shaver, G.
1187 R. and: Modelling the soil-plant-atmosphere continuum in a *Quercus-Acer* stand at Harvard
1188 Forest: the regulation of stomatal conductance by light, nitrogen and soil/plant hydraulic
1189 properties., *Plant Cell Environ.*, 19, 911–927, 1996.

1190

1191 Williams, M., Bond, B. and Ryan, M.: Evaluating different soil and plant hydraulic
1192 constraints on tree function using a model and sap flow data from ponderosa pine, *Plant Cell
1193 Amp Environ.*, 24, 679–690, 2001.

1194

1195 Woodward, F. I. and Lomas, M. R.: Vegetation dynamics - simulating responses to climate
1196 change., *Biol. Rev.*, 79, 643–670, 2004.

1197

1198 Xu, L. and Baldocchi, D. D.: Seasonal trends in photosynthetic parameters and stomatal
1199 conductance of blue oak (*Quercus douglasii*) under prolonged summer drought and high
1200 temperature, *Tree Physiol.*, 23, 865–877, 2003.

1201

1202 Zhou, S., Duursma, R. A., Medlyn, B. E., Kelly, J. W. and Prentice, I. C.: How should we
1203 model plant responses to drought? An analysis of stomatal and non-stomatal responses to
1204 water stress, *Agric. For. Meteorol.*, 182-183, 204–214, 2013.

1205

1206 Zhou, S., Medlyn, B., Sabaté, S., Sperlich, D. and Prentice, I. C.: Short-term water stress
1207 impacts on stomatal, mesophyll and biochemical limitations to photosynthesis differ
1208 consistently among tree species from contrasting climates, *Tree Physiol.*, 10, 1035–1046,
1209 2014.

1210

1211

1212

1213

1214

1215

1216

1217

1218

1219

1220

1221

1222

1223

Martin De Kauwe 7/12/2015 3:19 PM

Deleted: .

1225 **Figure Captions**

1226 Figure 1: A comparison of the observed (OBS) and modelled (CTRL) Latent Heat (LE) and
1227 transpiration (E) at five Fluxnet sites during 2003. The data have been smoothed with a 5-day
1228 moving window to aid visualisation.

1229
1230 Figure 2: Modelled impact of drought on the assimilation rate (A), shown as (a) a function of
1231 volumetric soil moisture content (θ) and (b) soil water potential (Ψ_s) for a sand and clay soil.

1232
1233 Figure 3: A comparison of the observed (OBS) and modelled latent Heat (LE), transpiration
1234 (E) and gross primary productivity (GPP) at the Tharandt site during 2003. Simulations show
1235 the control (CTRL) and the three parameterisations that represent a spectrum of behaviour
1236 ranging from a high to low drought sensitivity, and the tested methods to obtain a weighted
1237 estimate of soil water potential (Ψ_s) across CABLE's soil layers (M1-M3). M1 uses a root-
1238 biomass weighted soil water content converted to Ψ_s , M2 calculates Ψ_s by integrated soil
1239 water content over the top 1.7m of the soil, and M3 is calculated using a dynamic weight
1240 across soil layers. The data have been smoothed with a 5-day moving window to aid
1241 visualisation and the grey bars show daily rainfall.

1242
1243 Figure 4: A comparison of the observed (OBS) and modelled latent Heat (LE), transpiration
1244 (E) and gross primary productivity (GPP) at the Hesse site during 2003. Simulations show the
1245 control (CTRL) and the three parameterisations that represent a spectrum of behaviour
1246 ranging from a high to low drought sensitivity, and the tested methods to obtain a weighted
1247 estimate of soil water potential (Ψ_s) across CABLE's soil layers (M1-M3). M1 uses a root-
1248 biomass weighted soil water content converted to Ψ_s , M2 calculates Ψ_s by integrated soil
1249 water content over the top 1.7m of the soil, and M3 is calculated using a dynamic weight
1250 across soil layers. The data have been smoothed with a 5-day moving window to aid
1251 visualisation and the grey bars show daily rainfall.

1252

Martin De Kauwe 7/12/2015 3:19 PM

Deleted: -

... [1]

Martin De Kauwe 5/12/2015 9:59 AM

Deleted: A comparison of the observed (OBS) and modelled latent Heat (LE) and transpiration (E) at the Tharandt site during 2003. Simulations show the control (CTRL) and the three drought sensitivities to drought (high, medium, low) based on Zhou et al. (2013; 2014) and three different methods to calculate soil water potential (Ψ_s). The data have been smoothed with a 5-day moving window to aid visualisation. -

Martin De Kauwe 5/12/2015 10:02 AM

Deleted: A comparison of the observed (OBS) and modelled latent Heat (LE) and transpiration (E) at the Hesse site during 2003. Simulations show the control (CTRL) and the three drought sensitivities to drought (high, medium, low) based on Zhou et al. (2013; 2014) and three different methods to calculate soil water potential (Ψ_s). The data have been smoothed with a 5-day moving window to aid visualisation.

1275 Figure 5: A comparison of the observed (OBS) and modelled latent Heat (LE), transpiration
1276 (E) and gross primary productivity (GPP) at the Roccarespampani site during 2003.
1277 Simulations show the control (CTRL) and the three parameterisations that represent a
1278 spectrum of behaviour ranging from a high to low drought sensitivity, and the tested methods
1279 to obtain a weighted estimate of soil water potential (Ψ_s) across CABLE's soil layers (M1-
1280 M3). M1 uses a root-biomass weighted soil water content converted to Ψ_s , M2 calculates Ψ_s
1281 by integrated soil water content over the top 1.7m of the soil, and M3 is calculated using a
1282 dynamic weight across soil layers. The data have been smoothed with a 5-day moving
1283 window to aid visualisation and the grey bars show daily rainfall.

1284

1285 Figure 6: A comparison of the observed (OBS) and modelled latent Heat (LE), transpiration
1286 (E) and gross primary productivity (GPP) at the Castelporziano site during 2003. Simulations
1287 show the control (CTRL) and the three parameterisations that represent a spectrum of
1288 behaviour ranging from a high to low drought sensitivity, and the tested methods to obtain a
1289 weighted estimate of soil water potential (Ψ_s) across CABLE's soil layers (M1-M3). M1 uses
1290 a root-biomass weighted soil water content converted to Ψ_s , M2 calculates Ψ_s by integrated
1291 soil water content over the top 1.7m of the soil, and M3 is calculated using a dynamic weight
1292 across soil layers. The data have been smoothed with a 5-day moving window to aid
1293 visualisation and the grey bars show daily rainfall.

1294

1295 Figure 7: A comparison of the observed (OBS) and modelled latent Heat (LE), transpiration
1296 (E) and gross primary productivity (GPP) at the Espirra site during 2003. Simulations show
1297 the control (CTRL) and the three parameterisations that represent a spectrum of behaviour
1298 ranging from a high to low drought sensitivity, and the tested methods to obtain a weighted
1299 estimate of soil water potential (Ψ_s) across CABLE's soil layers (M1-M3). M1 uses a root-
1300 biomass weighted soil water content converted to Ψ_s , M2 calculates Ψ_s by integrated soil
1301 water content over the top 1.7m of the soil, and M3 is calculated using a dynamic weight
1302 across soil layers. The data have been smoothed with a 5-day moving window to aid
1303 visualisation and the grey bars show daily rainfall.

1304

Martin De Kauwe 5/12/2015 10:02 AM

Deleted: A comparison of the observed (OBS) and modelled latent Heat (LE) and transpiration (E) at the Roccarespampani site during 2003. Simulations show the control (CTRL) and the three drought sensitivities to drought (high, medium, low) based on Zhou et al. (2013; 2014) and three different methods to calculate soil water potential (Ψ_s). The data have been smoothed with a 5-day moving window to aid visualisation.

Martin De Kauwe 5/12/2015 10:11 AM

Formatted: Font:Not Italic

Martin De Kauwe 5/12/2015 10:11 AM

Formatted: Font:Not Italic

Martin De Kauwe 5/12/2015 10:11 AM

Formatted: Font:Not Italic

Martin De Kauwe 5/12/2015 10:02 AM

Deleted: A comparison of the observed (OBS) and modelled latent Heat (LE) and transpiration (E) at the Castelporziano Fluxnet site during 2003. Simulations show the control (CTRL) and the three drought sensitivities to drought (high, medium, low) based on Zhou et al. (2013; 2014) and three different methods to calculate soil water potential (Ψ_s). The data have been smoothed with a 5-day moving window to aid visualisation.

Martin De Kauwe 5/12/2015 10:03 AM

Deleted: A comparison of the observed (OBS) and modelled latent Heat (LE) and transpiration (E) at the Espirra site during 2003. Simulations show the control (CTRL) and the three drought sensitivities to drought (high, medium, low) based on Zhou et al. (2013; 2014) and three different methods to calculate soil water potential (Ψ_s). The data have been smoothed with a 5-day moving window to aid visualisation.

1335 Supplementary Figure 1: Simulated soil water content of each of CABLE's six layers for the
1336 control (CTRL), and three drought sensitivities (high, medium, low) based on Zhou et al.
1337 (2013; 2014) at the Tharandt site. The grey shading highlights the heatwave period between
1338 the 1st of June and the 31st of August. The data have been smoothed with a 5-day moving
1339 window to aid visualisation.

1340 Supplementary Figure 2: Simulated soil water content of each of CABLE's six layers for the
1341 control (CTRL), and three drought sensitivities (high, medium, low) based on Zhou et al.
1342 (2013; 2014) at the Hesse site. The grey shading highlights the heatwave period between the
1343 1st of June and the 31st of August. The data have been smoothed with a 5-day moving
1344 window to aid visualisation.

1345

1346

1347 Supplementary Figure 3: Simulated soil water content of each of CABLE's six layers for the
1348 control (CTRL), and three drought sensitivities (high, medium, low) based on Zhou et al.
1349 (2013; 2014) at the Roccarespampani site. The grey shading highlights the heatwave period
1350 between the 1st of June and the 31st of August. The data have been smoothed with a 5-day
1351 moving window to aid visualisation.

1352

1353 Supplementary Figure 4: Simulated soil water content of each of CABLE's six layers for the
1354 control (CTRL), and three drought sensitivities (high, medium, low) based on Zhou et al.
1355 (2013; 2014) at the Castelporziano site. The grey shading highlights the heatwave period
1356 between the 1st of June and the 31st of August. The data have been smoothed with a 5-day
1357 moving window to aid visualisation.

1358

1359 Supplementary Figure 5: Simulated soil water content of each of CABLE's six layers for the
1360 control (CTRL), and three drought sensitivities (high, medium, low) based on Zhou et al.
1361 (2013; 2014) at the Espirra site. The grey shading highlights the heatwave period between the
1362 1st of June and the 31st of August. The data have been smoothed with a 5-day moving

1363 window to aid visualisation.

1364

1365

1366

1367

1368

1369

1370

1371

1372

1373

1374

1375

1376

1377

1378

1379

1380

1381

1382

1383 Table 1. Baseline parameter values used to represent the three sensitivities: “high” (*Quercus*
 1384 *robur*), “medium” (*Quercus ilex*) and “low” (*Cedrus atlantica*) to drought stress. Parameter
 1385 values are taken from Zhou et al. (2013; 2014).

Sensitivity	b	S_f	Ψ_f
High	1.55	6.0	-0.53
Medium	0.82	1.9	-1.85
Low	0.46	5.28	-2.31

1386

1387 Table 2: Summary of flux tower sites.

Site	PFT	Dominant species	Latitude	Longitude	Country	Sand/Silt/Clay Fraction
Tharandt	ENF	<i>Picea abies</i>	50°58' N	13°34' E	Germany	0.37/0.33/0.3
Hesse	DBF	<i>Fagus sylvatica</i>	48°40' N	7°05' E	France	0.37/0.33/0.3
Roccarespampani	DBF	<i>Quercus cerris</i>	42°24' N	11°55' E	Italy	0.6/0.2/0.2
Castelporziano	EBF	<i>Quercus ilex</i>	41°42' N	12°22' E	Italy	0.6/0.2/0.2
Espirra	EBF	<i>Eucalyptus globulus</i>	38°38' N	8°36' W	Portugal	0.37/0.33/0.3

1388

1389

1390

1391

1392

1393

1394

1395

1396 Table 3: Mean change in climate and fluxes between 2002 and 2003 covering the period
1397 between June and September.

Site	Precipitation (mm month ⁻¹)	Air temperature (° C)	GPP (g C m ⁻² month ⁻¹)	LE (W m ⁻²)
Tharandt	-115.57	1.45	-38.45	0.52
Hesse	-49.20	2.98	-123.38	-11.90
Roccarespampani	-87.36	2.18	-71.94	-6.17
Castelporziano	-20.31	4.57	-49.73	-6.47
Espirra	-14.45	1.77	28.46	22.83

1398

1399

1400

1401

1402

1403 Table 4: Summary statistics of modelled and observed latent heat (LE) at the five FLUXNET sites during the main drought period (1st of
1404 June – 31st August, 2003). The results of the three parameterisations, which represent a spectrum of behaviour, ranging from high to low
1405 drought sensitivity, are shown for the three tested approaches (M1-M3) to obtain a weighted estimate of soil water potential (Ψ_s) across
1406 CABLE's soil layers. M1 uses a root-biomass weighted soil water content converted to Ψ_s , M2 calculates Ψ_s by integrated soil water content
1407 over the top 1.7m of the soil, and M3 is calculated using a dynamic weighting across soil layers. Sites have been ordered to show a mesic-
1408 xeric transition between sites (Tharandt to Espirra). For each site the best performing model simulation has been highlighted in bold.

Site	Ψ_s Method	Root Mean Squared Error (RMSE; W m ⁻²)				Nash-Sutcliffe efficiency (NSE)				Pearsons's correlation coefficient (r)			
		CTRL	High	Medium	Low	CTRL	High	Medium	Low	CTRL	High	Medium	Low
Tharandt	<u>M1</u>	21.25	24.64;	26.57	29.55	-0.70	-1.28	-1.65	-2.28	0.69	0.73	0.73	0.70
	<u>M2</u>		34.59	36.20	36.97		-3.50	-3.93	-4.14		0.58	0.56	0.55
	<u>M3</u>		25.90	29.39	32.26		-1.52	-2.25	-2.94		0.72	0.67	0.63
Hesse	<u>M1</u>	28.50	36.22	41.59	51.49	0.15	-0.37	-0.81	-1.77	0.68	0.66	0.74	0.79
	<u>M2</u>		52.60	59.87	63.46		-1.89	-2.75	-3.21		0.80	0.75	0.71
	<u>M3</u>		28.82	45.32	56.46		0.13	-1.15	-2.33		0.79	0.84	0.77
Roccarespampani	<u>M1</u>	38.00	48.41	40.98	34.27	-0.34	-1.17	-0.55	-0.09	0.67	0.52	0.67;	0.81
	<u>M2</u>		31.62	22.81	26.81		0.08	0.52	0.34		0.83	0.84;	0.79
	<u>M3</u>		45.12	18.27	29.50		-0.88	0.69	0.20		0.67	0.85	0.81
Castelporziano	<u>M1</u>	31.76	38.77	40.54	40.40	-8.95	-13.82	-15.21	-15.10	0.18	-0.08	0.01	0.06
	<u>M2</u>		31.04	27.19	19.72		-8.50	-6.29	-2.84		0.47	0.54	0.57
	<u>M3</u>		39.17	20.47	20.41		-14.40;	-3.13	-3.11		-0.02	0.55	0.61

Espirra	<u>M1</u>	35.31	41.52	40.97	33.87	-3.35	-5.02;	-4.86	-3.01;	0.42	0.32	0.59	0.70
	<u>M2</u>		15.58	13.82	13.84		0.15;	0.33	0.33;		0.77	0.74	0.73
	<u>M3</u>		41.01	20.41	15.40		-4.81	-0.45	0.17		0.57	0.53	0.55

1409

1410

1411

1412

1413

1414

1415

1416

1417 Table 5: Summary statistics of modelled and flux derived gross primary productivity (GPP) at the five FLUXNET sites during the main
 1418 drought period (1st of June – 31st August, 2003). The results of the three parameterisations, which represent a spectrum of behaviour, ranging
 1419 from high to low drought sensitivity, are shown for the three tested approaches (M1-M3) to obtain a weighted estimate of soil water potential
 1420 (Ψ_s) across CABLE's soil layers. M1 uses a root-biomass weighted soil water content converted to Ψ_s , M2 calculates Ψ_s by integrated soil
 1421 water content over the top 1.7m of the soil, and M3 is calculated using a dynamic weighting across soil layers. Sites have been ordered to
 1422 show a mesic-xeric transition between sites (Tharandt to Espirra). For each site the best performing model simulation has been highlighted in
 1423 bold.

Martin De Kauwe 7/12/2015 3:14 PM

Deleted: observed

Site	Ψ_s Method	Root Mean Squared Error (RMSE; g C m ⁻² d ⁻¹)				Nash-Sutcliffe efficiency (NSE)				Pearsons's correlation coefficient (r)			
		CTRL	High	Medium	Low	CTRL	High	Medium	Low	CTRL	High	Medium	Low
Tharandt	<u>M1</u>	2.06	2.27	2.07	2.10	0.33	0.19	0.33	0.31	0.80	0.71	0.66	0.61
	<u>M2</u>		2.25	2.29	2.30		0.20	0.18	0.17		0.52	0.51	0.50
	<u>M3</u>		2.23	2.12	2.20		0.22	0.30	0.25		0.66	0.59	0.55
Hesse	<u>M1</u>	2.85	3.57	2.48	2.94	0.48	0.18	0.60	0.44	0.79	0.78	0.78	0.71
	<u>M2</u>		2.65	3.22	3.47		0.55	0.33	0.22		0.75	0.67	0.62
	<u>M3</u>		3.51	2.71	3.24		0.21	0.53	0.32		0.83	0.75	0.66
Roccarespampani	<u>M1</u>	2.49	3.70	2.69	2.38	0.42	-0.28	0.32	0.47	0.85	0.64	0.82	0.87
	<u>M2</u>		2.12	1.47	2.84		0.58	0.80	0.24		0.92	0.91	0.87
	<u>M3</u>		3.74	1.73	3.08		-0.31	0.72	0.11		0.84	0.91	0.85
Castelporziano	<u>M1</u>	2.22	3.46	3.64	3.76	-2.16	-6.71	-7.51	-8.08	0.55	-0.18	0.07	0.13
	<u>M2</u>		2.65	1.84	1.22		-3.52	-1.17	0.04		0.63	0.63	0.81
	<u>M3</u>		3.71	0.95	1.46		-7.82	0.42	-0.37		0.05	0.81	0.84
Espirra	<u>M1</u>	3.03	4.39	4.33	3.72	-2.67	-6.72	-6.51	-4.55	0.74	0.58	0.53	0.67

1425

<u>M2</u>	1.92	1.46	1.34	-0.48	0.14	0.28	0.80	0.81	0.81
<u>M3</u>	4.70	2.01	1.43	-7.84	-0.62	0.18	0.34	0.74	0.78

Figure 1

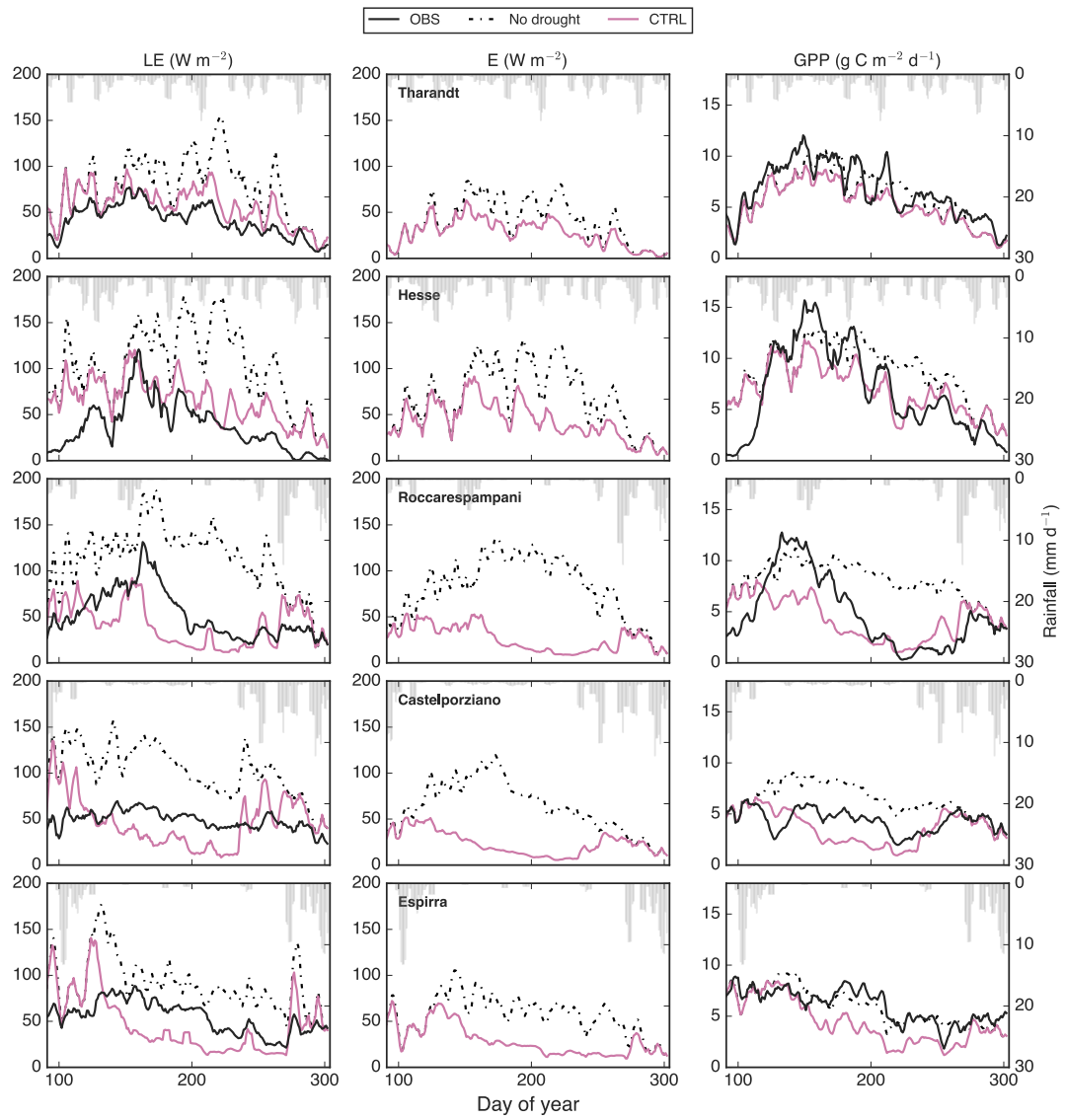


Figure 2

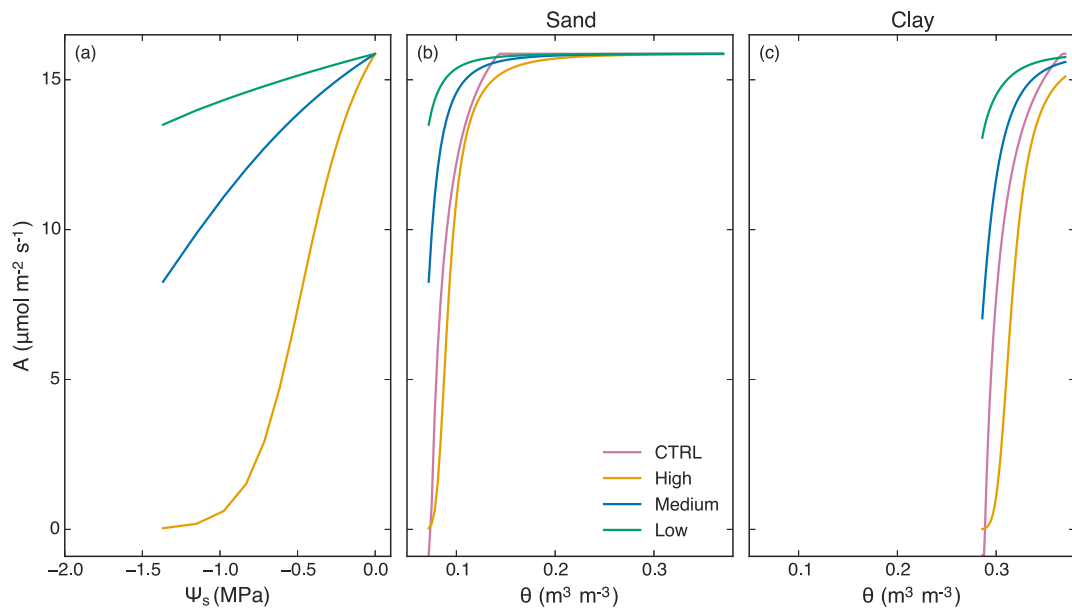


Figure 3

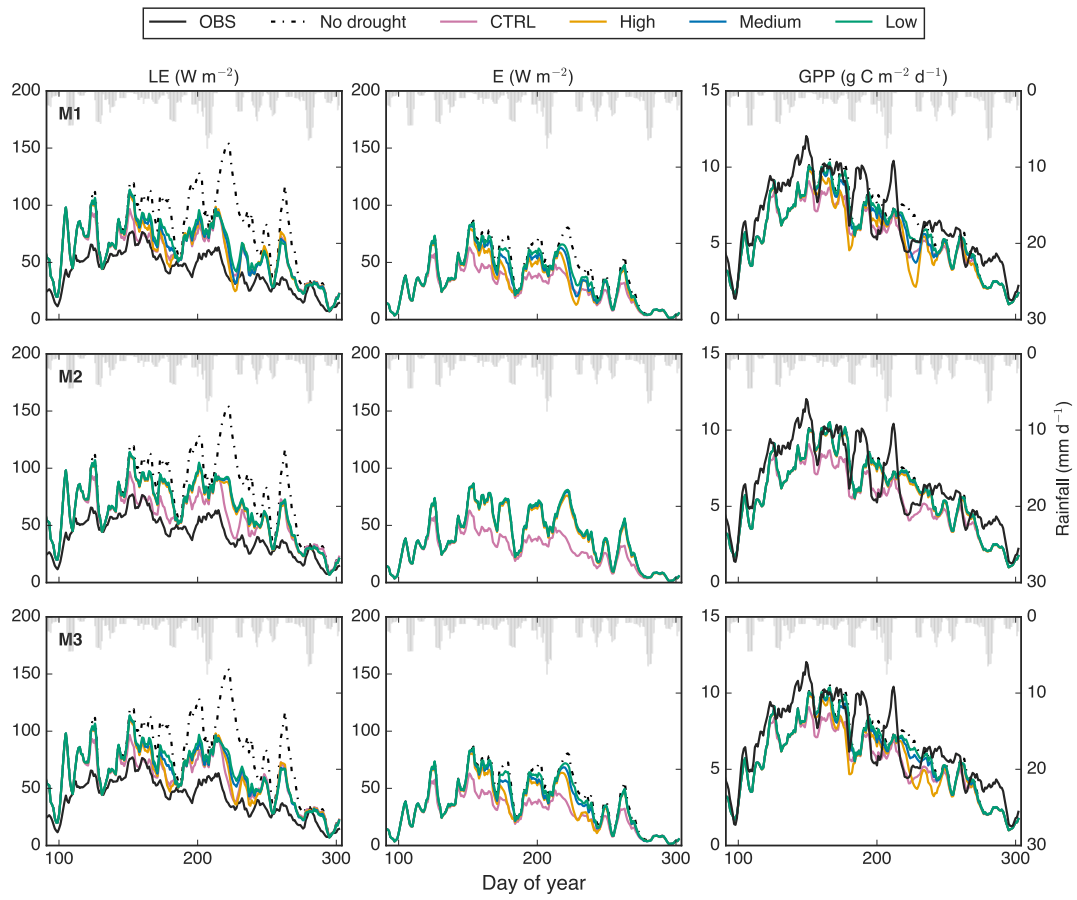


Figure 4

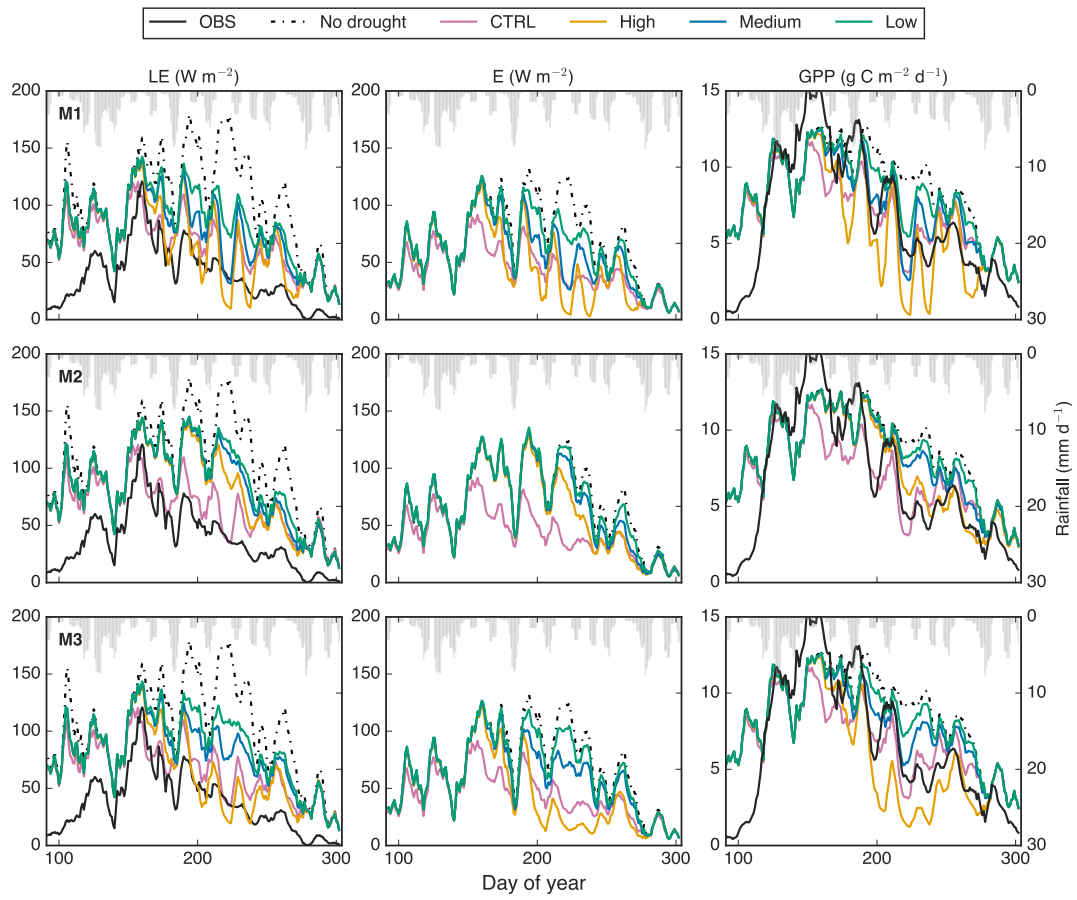


Figure 5

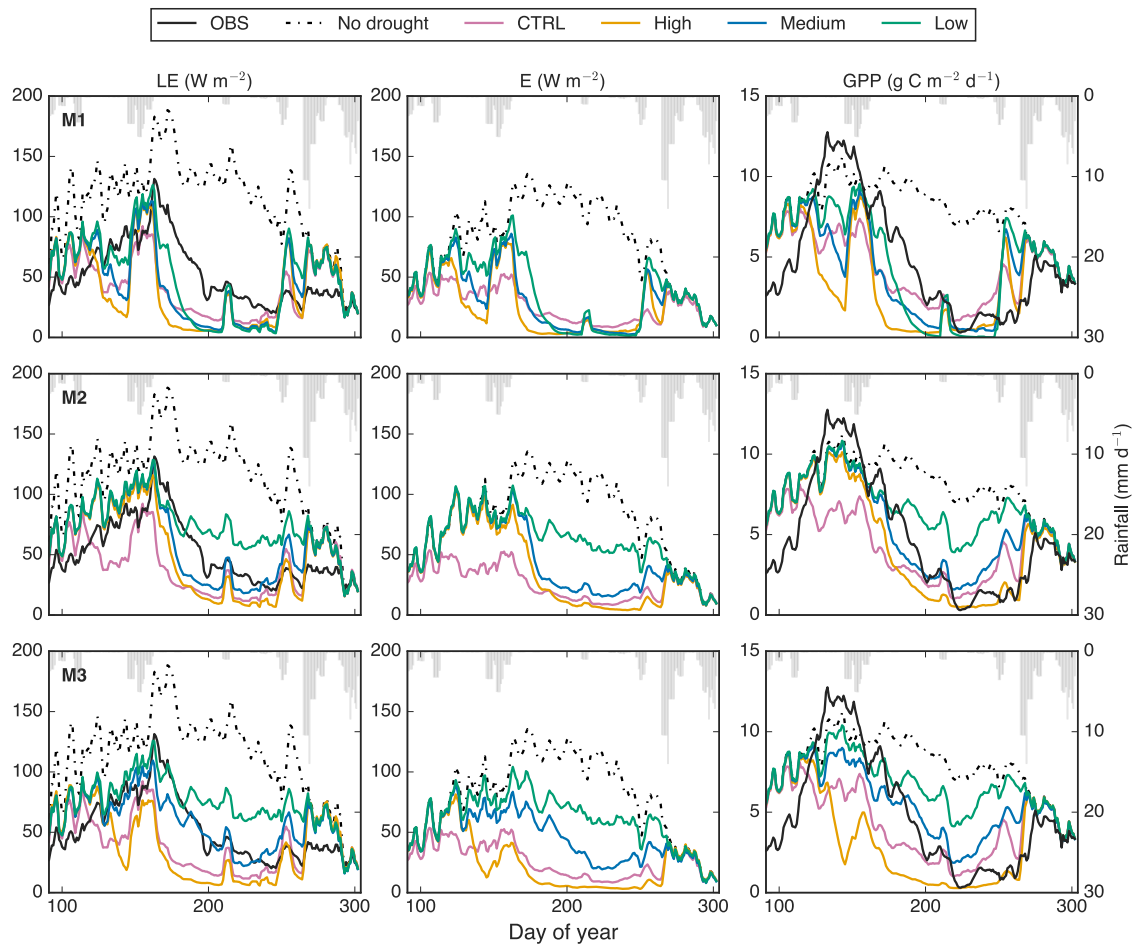


Figure 6

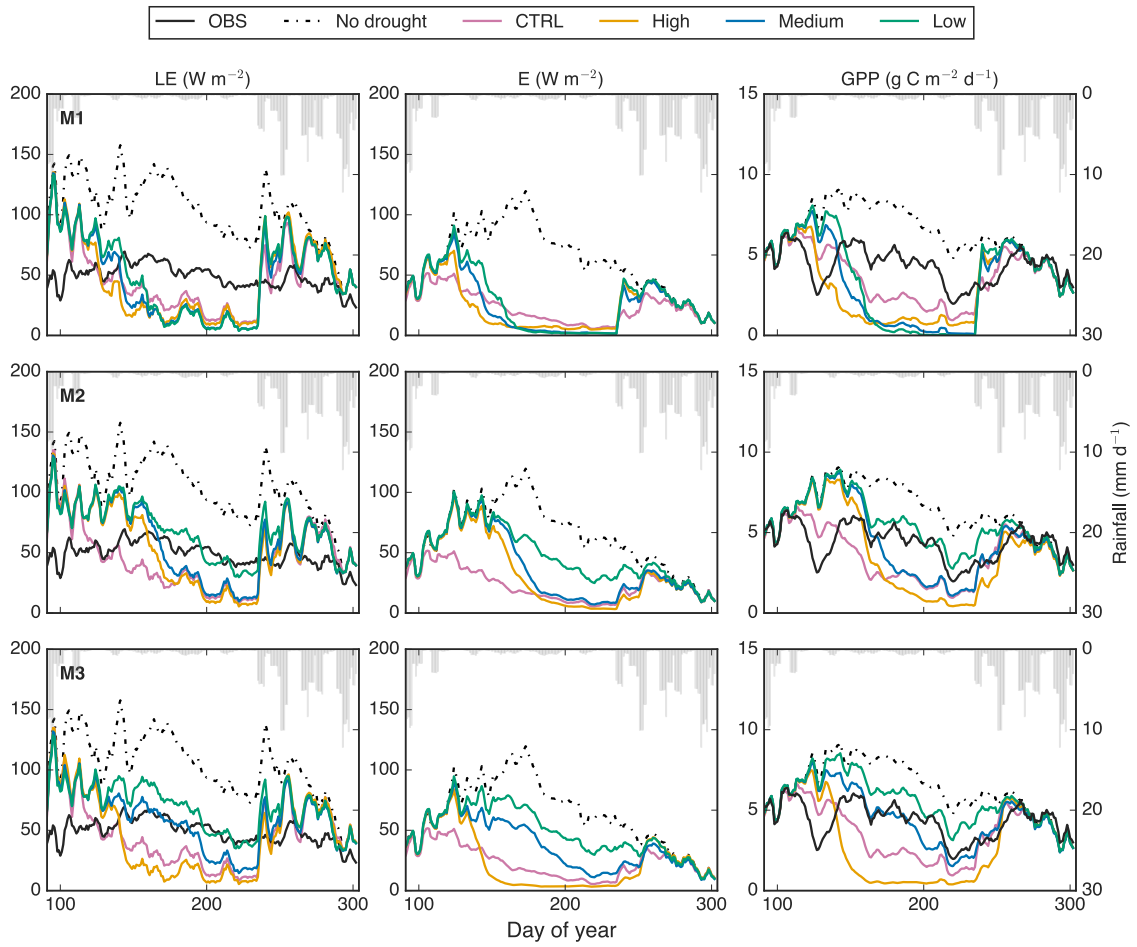


Figure 7

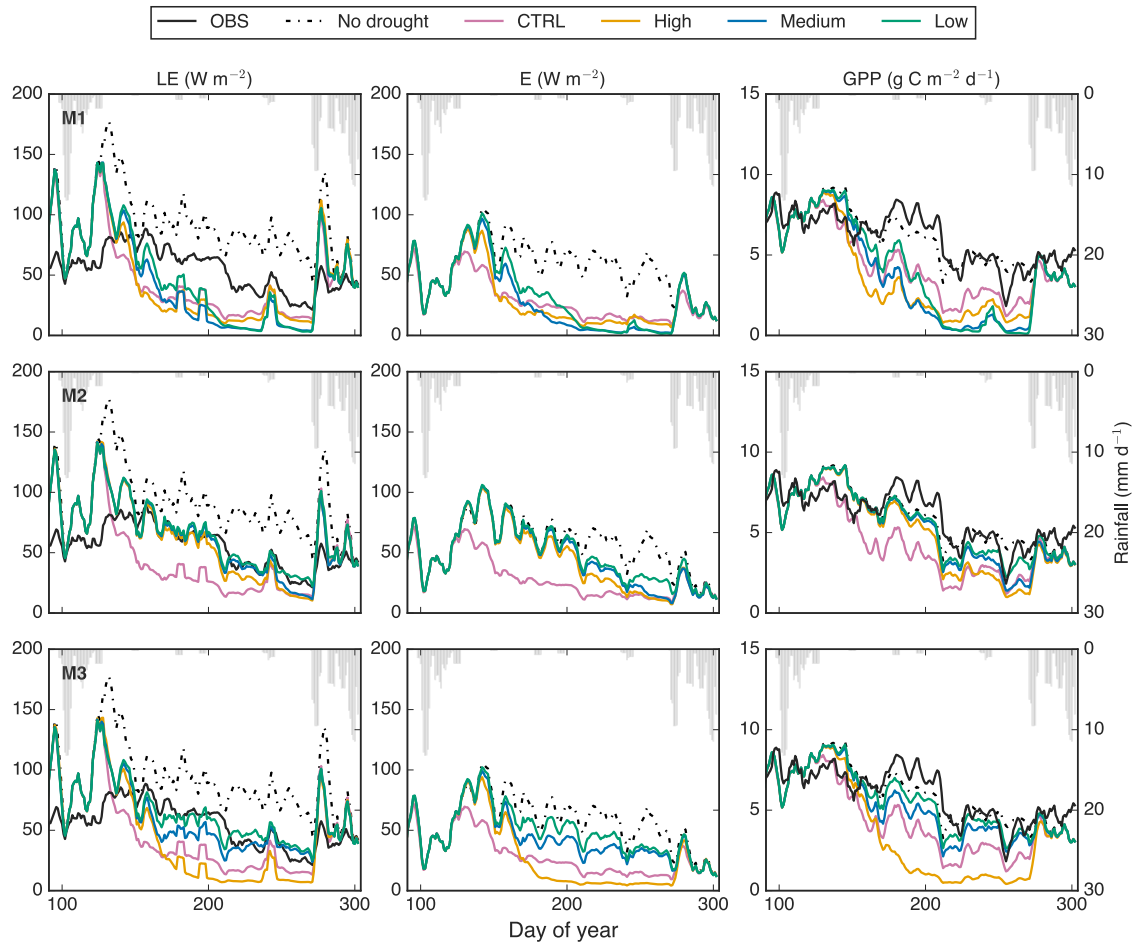


Figure S1

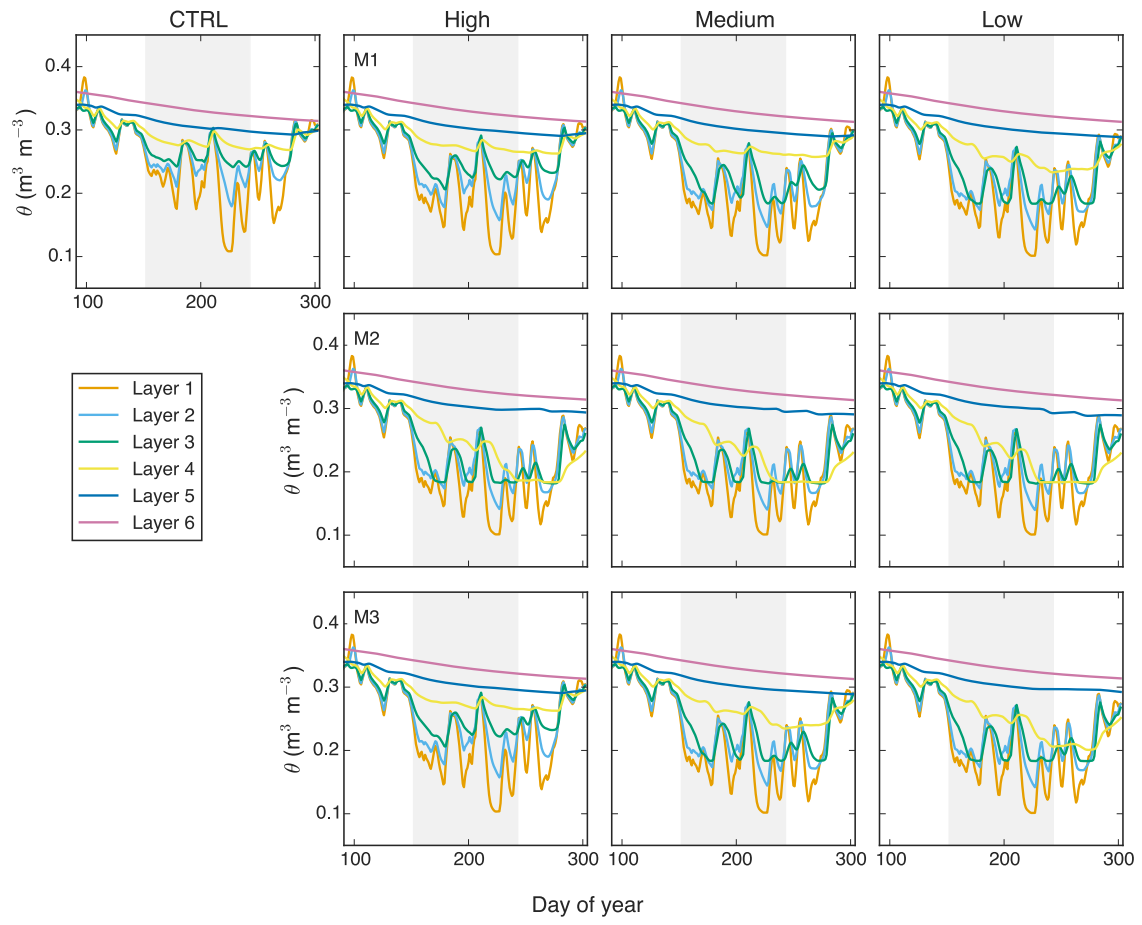


Figure S2

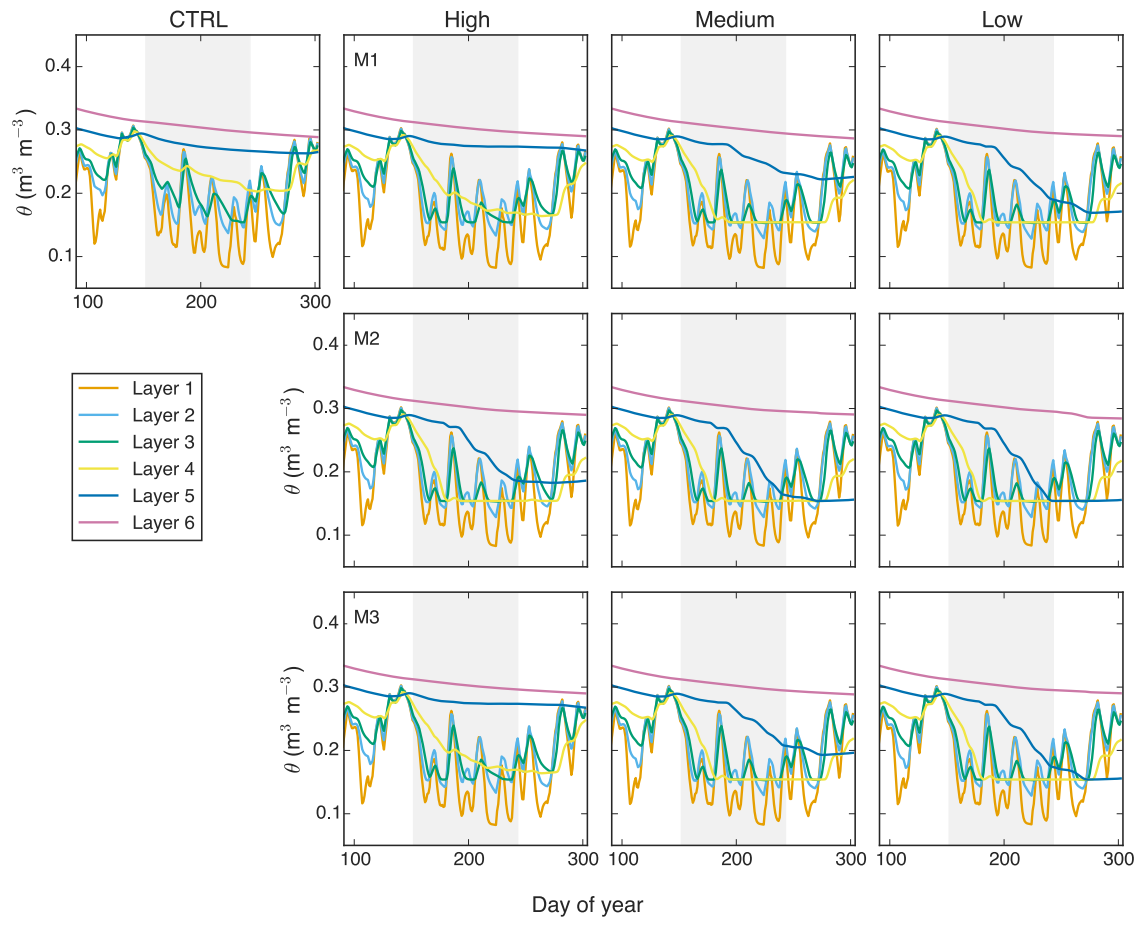


Figure S3

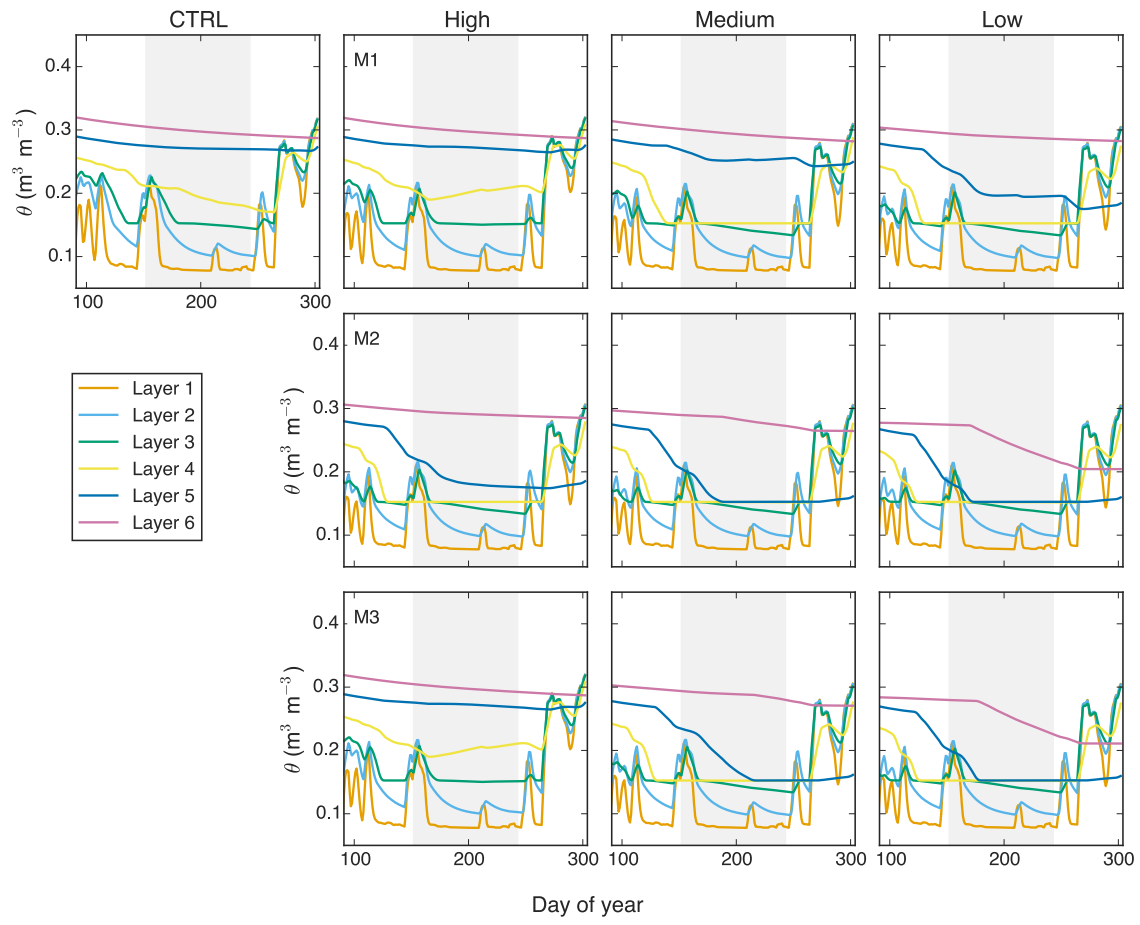


Figure S4

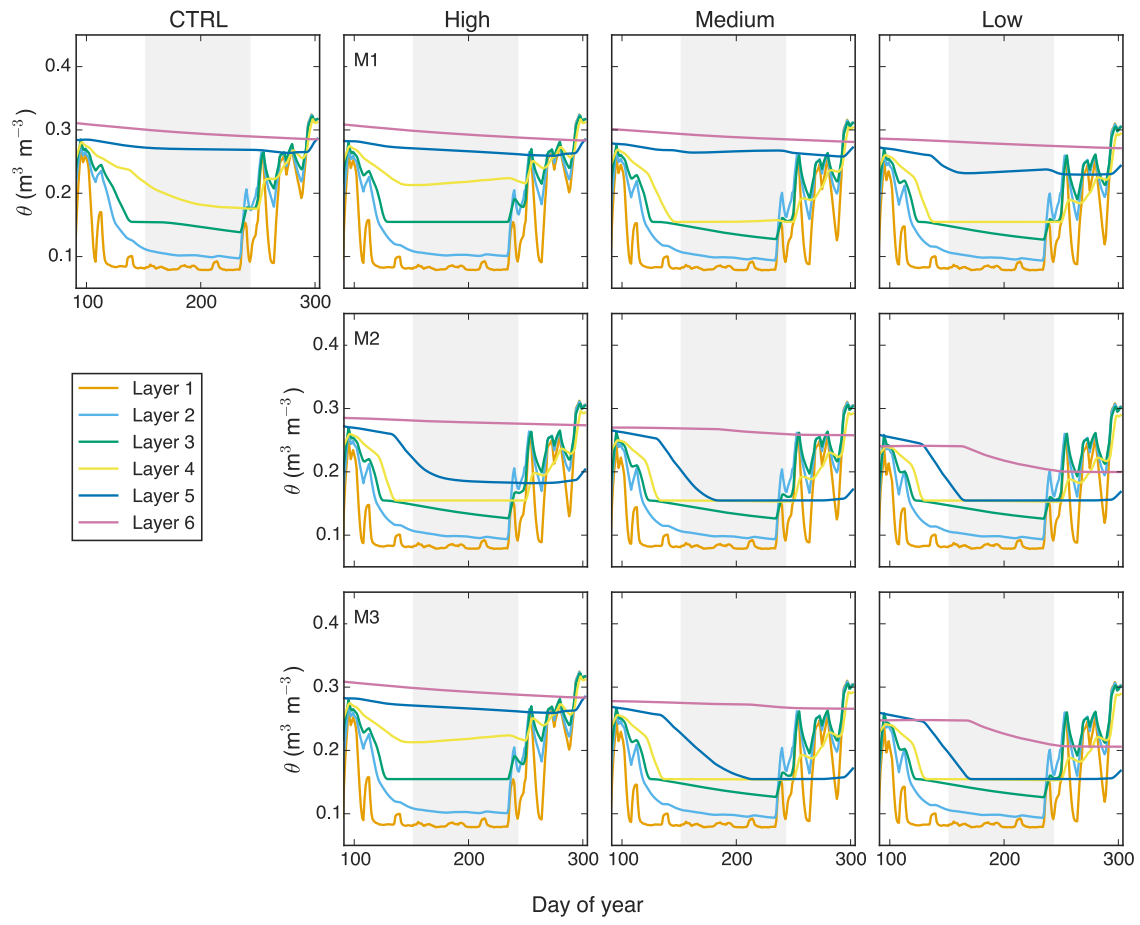


Figure S5

